

Comparison of granite-related uranium deposits in the Beaverlodge district (Canada) and South China – A common control of mineralization by coupled shallow and deep-seated geologic processes in an extensional setting

Guoxiang Chi^{a,*}, Kenneth Ashton^b, Teng Deng^c, Deru Xu^c, Zenghua Li^c, Hao Song^d, Rong Liang^a, Jacklyn Kennicott^a

^a Department of Geology, University of Regina, Regina, Saskatchewan, Canada

^b Saskatchewan Geological Survey, Regina, Saskatchewan, Canada

^c State Key Laboratory of Nuclear Resources and Environment, East China University of Technology, Nanchang, China

^d Key Laboratory of Sichuan Province of Applied Nuclear Technology in Geosciences, Chengdu University of Technology, Chengdu, China



ARTICLE INFO

Keywords:

Granite-related
Uranium deposits
Beaverlodge
South China
Red bed basin
Coupled control

ABSTRACT

Many uranium deposits are related to granitic rocks, but the mineralization ages are much younger, thus excluding a direct magmatic-hydrothermal link between the mineralization and the granites. Two such examples are the Proterozoic “vein-type” uranium deposits in the Beaverlodge district in Canada and the Mesozoic granite-related uranium deposits in South China. Both areas have been extensively studied, but the critical factors that control the mineralization remain unclear.

The uranium mineralization in the Beaverlodge district occurs in quartz – carbonate ± albite veins and breccias developed within and near major deformation zones, and are mainly hosted by ca. 2.33 – 1.90 Ga granitic rocks and ca. 2.33 Ga Murmac Bay Group amphibolite. These rocks are unconformably overlain by the Martin Lake Basin, which was formed during a period of regional extension in the later stage of the Trans-Hudson orogeny and is filled with red beds. A ca. 1820 Ma mafic magmatic event is manifested as volcanic rocks occurring within the Martin Lake Basin and as dikes crosscutting the basement rocks and lower Martin Group strata. Uraninite U-Pb and Pb-Pb ages range from ca. 2290 Ma to < 300 Ma, with a peak overlapping the mafic magmatism.

The granite-related uranium mineralization in South China occurs mainly as quartz – carbonate ± fluorite veins and as disseminations in the host rocks adjacent to fracture zones. The deposits are hosted by, or occur adjacent to, granitic rocks, and are spatially close to Cretaceous – Tertiary red bed basins that were formed in a Basin-and-Range like tectonic setting related to roll back of the Pacific plate. These red bed basins contain intervals of bimodal volcanic rocks and are crosscut by coeval mafic dikes. Uraninite U-Pb ages dominantly range from 100 to 50 Ma, which is much younger than the host granites (> 145 Ma) and broadly contemporaneous with development of the red bed basins and mafic magmatism.

Comparison of the two study areas reveals striking similarities in geologic attributes related to uranium mineralization, specifically, the development of large volumes of granitic rocks that are relatively enriched in uranium, and the development of red bed basins with accompanying coeval mafic magmatism in extensional tectonic settings. It is proposed that oxidizing basinal fluids from the red bed basins circulated into the underlying fertile granitic rocks along high-permeability structural zones, acquired uranium in the path through fluid-rock interaction, and precipitated the uranium where they encountered reducing agents. Elevated geothermal gradients associated with the mantle-derived magmatism greatly enhanced the mineralization by facilitating the uranium extraction and transport processes. Thus, it is the coupling of shallow (red bed basin and oxidizing basinal fluid development) and deep-seated (mantle-derived magmatism and related thermal activity) processes, together with the pre-enrichment of uranium in basement rocks (particularly granitic rocks) and pre-existing deformation zones, that controlled the formation of the granite-related uranium deposits in both Beaverlodge and South China, and perhaps elsewhere in the world with similar geologic setting.

* Corresponding author.

E-mail address: guoxiang.chi@uregina.ca (G. Chi).

<https://doi.org/10.1016/j.oregeorev.2020.103319>

Received 28 August 2019; Received in revised form 29 November 2019; Accepted 7 January 2020

Available online 09 January 2020

0169-1368/ © 2020 Elsevier B.V. All rights reserved.

1. Introduction

Granite-related uranium deposits are those that are spatially associated with granitic intrusions, including ‘veins composed of ore and gangue minerals in granite or adjacent (meta)sediments, and disseminated mineralization in episyenite bodies internal to the granite that are commonly gradational to veins’ (IAEA, 2018). These deposits were a major contributor to the world’s uranium production until the 1950’s, when uranium deposits associated with sedimentary basins became the dominant uranium producer (Ruzicka, 1993). Granite-related uranium deposits are mainly distributed in the Variscan orogens in Europe (especially in France, Germany, Czech, Spain and Portugal) and in Yanshanian (Jurassic to Cretaceous) orogens in South China (Du and Wang, 1984; Ruzicka, 1993; Huang et al., 1994; Hu et al., 2008; Dahlkamp, 2009; IAEA, 2009, 2018; Zhang et al., 2019), the latter remaining as an important uranium producer in China up to present day. Most of the uranium deposits in the Proterozoic Beaverlodge uranium district in northern Saskatchewan (Canada) are located within or adjacent to granitic rocks, and can be classified as granite-related uranium deposits, although they have been given different names in the past, including “vein uranium deposits” (Ruzicka, 1993), “metasomatic deposits” (IAEA, 2009), and “structure-bound deposits” under the class of “metamorphite deposits” (IAEA, 2018).

The mineralization ages of the majority of the granite-related uranium deposits are significantly younger than the granites that host, or are adjacent to, the uranium mineralization (Du and Wang, 1984; Ruzicka, 1993; Hu et al., 2008; Dahlkamp, 2009; IAEA 2009, 2018; Zhang et al., 2019). This implies that the majority of the uranium mineralization is not directly related to the magmatic-hydrothermal fluids emanating from the granitic intrusions, even though the latter may have served as a uranium source at a later time. Although granites with similar compositions to those hosting or adjacent to the uranium mineralization are well developed in many orogenic belts in many different parts of the world, granite-related uranium mineralization appears to be concentrated in several districts. This has led geologists to question the geological factors that determine whether or not uranium deposits will be formed in a given area characterized by development of granites. This paper aims to tackle this question through comparison of granite-related uranium deposits in the Beaverlodge district in Canada and those in South China, based on a review of geological, geochemical and geochronological data from both regions. The common geological factors from the two regions, despite their large difference in geological time, are analyzed to determine their roles in controlling uranium mineralization.

2. Uranium mineralization in the Beaverlodge district

2.1. Geological setting

The Beaverlodge district is located on the north shore of Lake Athabasca in northern Saskatchewan, within the southwestern Rae Subprovince (or Rae craton) in the Churchill Province (Fig. 1a). The Churchill Province is divided into the Rae Subprovince and the Hearne Subprovince (or Hearne craton) along the Snowbird Tectonic Zone (Fig. 1a) (Hoffman, 1988). The Rae Subprovince is separated from the Slave Province by the Thelon Orogen to the west and is fringed by the Taltson Orogen in the southwest, whereas the Hearne Subprovince is flanked by the Trans-Hudson Orogen to the east (Fig. 1a) (Hoffman, 1988; Card et al., 2007). The Rae Subprovince in northern Saskatchewan is divided into several domains, including Nolan, Zemplak, Beaverlodge, Train Lake, Dodge and Tantato (Fig. 1b).

The rocks in the Beaverlodge district (Fig. 1c) comprise granitoids of Archean and Paleoproterozoic ages and supracrustal rocks of Paleo- to Mesoproterozoic ages. The granitic rocks include ca. 3.0 Ga granitoids and orthogneisses derived from them, ca. 2.62 to 2.60 Ga granodiorites and granites (Hartlaub et al., 2004, 2005), ca. 2.33 to 2.29 Ga granites

(Hartlaub et al., 2007), and ca. 1.94 to 1.90 Ga granites and leucogranites (Ashton et al., 2013a,b). The supracrustal rocks include the ca. 2.33 to < 2.00 Ga Murmac Bay Group, ca. 1.82 Ga Martin Group, and ca. 1.75 to 1.50 Ga Athabasca Group (Ashton et al., 2013a,b). The Murmac Bay Group consists of amphibolite-facies metamorphic rocks comprising basal quartzite and/or psammite with intercalated dolostone, patchy iron formation, mafic volcanic flows, and overlying psammopelite – pelite (Tremblay, 1978; Hartlaub et al., 2004; Ashton et al., 2013b). The Martin Group, which lies unconformably upon the Murmac Bay Group and basement granitoids, consists of continental red beds (Tremblay, 1972; Mazimhaka and Hendry, 1984) and contains mafic volcanic rocks that are related to the ca. 1820 Ma mafic dikes in the area (Morelli et al., 2009). The Martin Group has undergone open folding and faulting, but has not been metamorphosed. The Athabasca Group was unconformably deposited upon the Murmac Bay Group and consists of flat-lying, unmetamorphosed sedimentary rocks mainly composed of quartz sandstone (Tremblay, 1978; Ramaekers et al., 2007).

The Archean-aged (ca. 3.0–2.6 Ga) rocks in the Beaverlodge domain are widespread in other parts of the Rae craton (Hartlaub et al., 2004, 2005), and were intruded by a number of Paleoproterozoic granitoids. The ca. 2.33–2.29 Ga granitoids and associated ca. 2.37–2.34 Ga metamorphism are attributed to the Arrowsmith orogeny that resulted from accretion of a terrane to the western Rae craton margin (Berman et al., 2005, 2013). The ca. 2.33 to < 2.00 Ga Murmac Bay Group, which is considered to be largely equivalent to the Amer and Ketyet River groups in the central Rae Province (Fig. 1A), may have been deposited in an intracontinental rift basin after the peak Arrowsmith orogeny. This rift basin gradually deepened with time (Rainbird et al., 2010) or switched to a foreland basin associated with a subsequent accretionary event at ca. 2.2–2.1 Ga (Ashton et al., 2013a,b). The ca. 1.94 to 1.90 Ga granites – leucogranites and associated metamorphism may be related to two consecutive and overlapping orogenic events focused on opposite sides of the craton, i.e., the ca. 1.94 – 1.92 Ga Taltson orogeny affecting the western margin of the Rae craton (Ashton et al., 2009; Bethune et al., 2013), and the ca. 1.91 – 1.90 Ga Snowbird orogeny associated with the collision between the Rae craton and Hearne craton to the east (Hoffman, 1988; Berman et al., 2007). The uranium concentrations in the granites may range from 1 to 13 ppm, which are considerably higher than those in the amphibolite (0.3 – 2.7 ppm) (Tremblay, 1972). A more recent study of leucogranites in the district yielded U concentrations from 2.9 to 48.7 ppm (with one outlier of 180 ppm) (LeGault, 2014).

The ca. 1.82 Ga Martin Group was deposited in an intracontinental basin (the Martin Lake Basin) during the waning stage of the ca. 1.9–1.8 Ga Trans-Hudson orogeny (Mazimhaka and Hendry, 1984; Ashton et al., 2001, 2009; Morelli et al., 2009), and has been suggested to be correlative with the Baker Lake Group of the Dubawnt Supergroup in Nunavut in the central Rae craton (Ashton et al., 2009) (Fig. 1a). The volcanic rocks within the Martin Group and regionally extensive mafic dikes have similar compositions ranging from subalkaline (tholeiitic) basalts to alkali basalts or trachyandesites, which show geochemical characteristics of enriched mantle that may have been inherited from precursor plate subduction (Morelli et al., 2009). Enriched mantle signatures have also been observed for the alkaline volcanic rocks in the Baker Lake Group and for coeval lamprophyre dikes in the region and linked to precursor plate subduction, but it is highly uncertain which orogenic events they may be related to, with possibilities ranging from Archean, Arrowsmith, Taltson – Thelon, Snowbird, to Trans-Hudson orogenies (Ashton et al., 2009; Morelli et al., 2009). Although the Martin Lake Basin may have been initiated as a pull-apart basin in a W-E transpressional stress regime (Mazimhaka and Hendry, 1984; Ashton et al., 2001, 2009), the extensive development of mantle-derived magmatism associated with fault-controlled basins across a large area from the central to southwestern Rae craton (Fig. 1a) is likely related to a period of regional extension (Peterson et al., 2002; Ashton et al.,

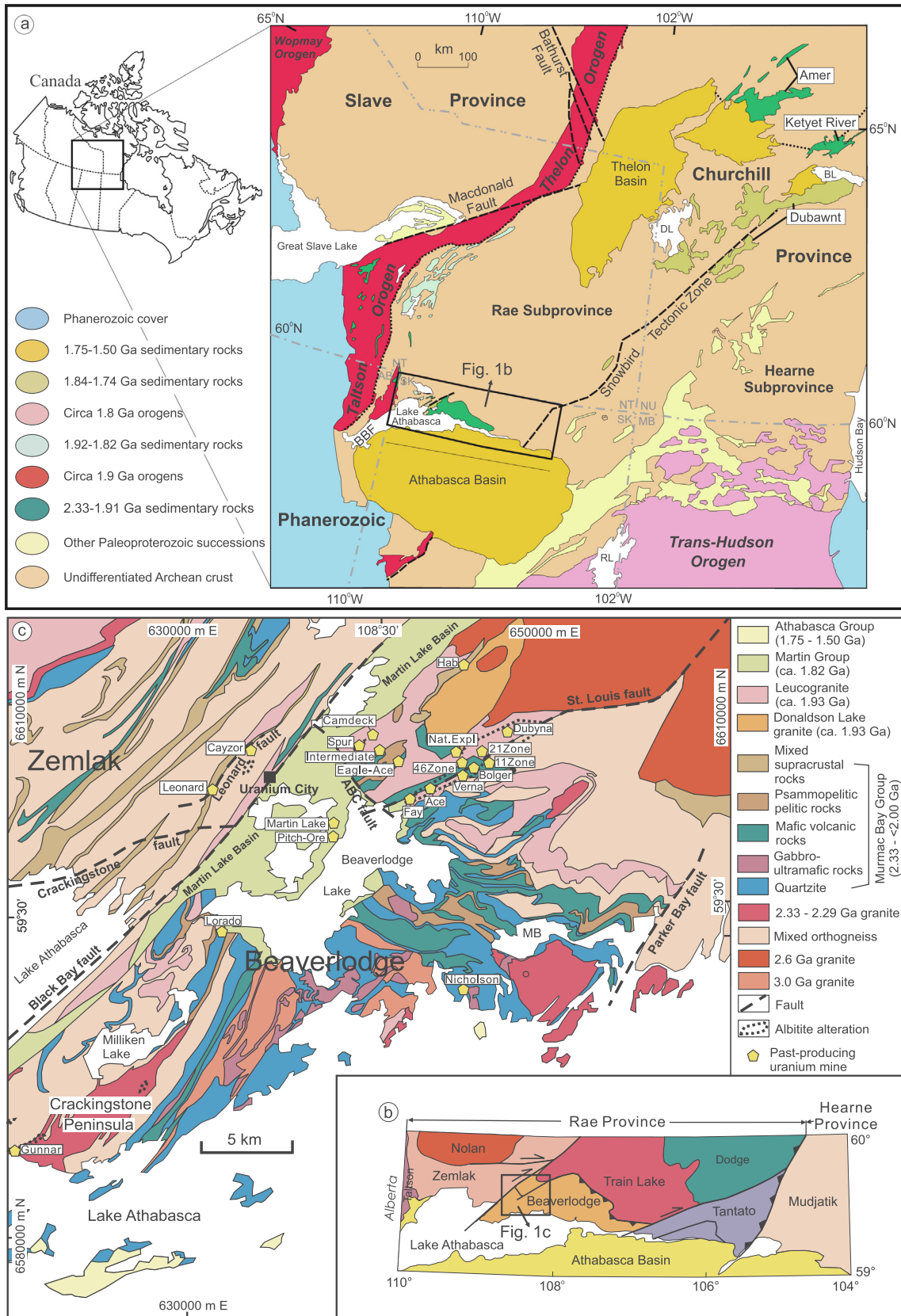


Fig. 1. (a) Regional geological map showing the location of northern Saskatchewan (Fig. 1b) (modified from Ashton et al., 2013b); (b) Sketch map showing the tectonic domains and location of the study area (Fig. 1c) in northern Saskatchewan (modified from Ashton et al., 2013a); (c) Geological map of the Beaverlodge district showing basic geological units and locations of uranium deposits/occurrences (modified from Ashton et al., 2013a).

2018). Nevertheless, the folding of the Martin Group as well as the dextral displacement along the Black Bay and St. Louis faults (Fig. 1c) indicate a compressional or transpressional stress regime (Ashton et al., 2001, 2009), suggesting that the extensional tectonic setting was postdated by another episode of compressional regime in the later stage of the Trans-Hudson orogeny.

The ca. 1.75 – 1.5 Ga Athabasca Group in the Athabasca Basin is broadly synchronous with the Barrenland Group (mainly in the Thelon Basin) of the Dubawnt Supergroup in the central Rae craton (Fig. 1a; Rainbird et al., 2010). The Athabasca Basin and Thelon Basin are generally considered as intracratonic basins that developed following the Proterozoic assembly of Laurentia (Hoffman, 1988; Ramaekers et al., 2007), although the upper part of the basins may be related to the initiation of rifting that eventually led to the breakup of the Nuna supercontinent (Ramaekers et al., 2017).

2.2. Geological characteristics of uranium mineralization

The Beaverlodge district was historically an important uranium mining camp, having produced a total of 25,939 tonnes U_3O_8 grading 0.15%–0.25% U from 17 uranium deposits between 1953 and 1982 (Robinson, 1955; Beck, 1969, 1986; Tremblay, 1972; Jefferson et al., 2007). The most important uranium ore producers were the Fay – Ace – Verna mine and the Gunnar mine (Fig. 1c).

Most of the uranium deposits are hosted in the basement rocks of the Martin Lake Basin, although minor amounts of mineralization occur within the basin (Fig. 1c). Most of the deposits are located in or near faults developed within the basement, especially the St. Louis fault (Fig. 1c), and are spatially close to the edge of the residual Martin Lake Basin (Fig. 1c). The majority of the deposits are located within or adjacent to granitic rocks, especially leucogranites (Fig. 1c), although the immediate host rocks of mineralization may be non-granitic rocks, especially amphibolite of the Murmac Bay Group.

The uranium mineralization occurs in breccias, stockworks, disseminations, and veins associated with faults and fractures (Tremblay, 1972; Beck, 1986; Smith, 1986). Although the mineralization in the Beaverlodge district has been historically labelled as “vein-type” (Ruzicka, 1993), and vein-style mineralization is indeed the most common in terms of occurrences, the other styles of mineralization, especially breccia-type, are actually the most important in terms of ore tonnages (Tremblay, 1972). Although the veins were observed to locally crosscut other types of ores and the vein-style mineralization is mainly developed further away from the faults than the breccia ores (Robinson, 1955; Beck, 1969; Tremblay, 1972), the different types of ores may be considered to have been formed generally simultaneously (Liang et al., 2017). The majority of the veins are subvertical (Fig. 2c; Liang et al., 2017), which is consistent with an overall extensional tectonic setting (Liang et al., 2017).

Most of the uranium deposits are characterized by a relatively simple ore mineral assemblage, with pitchblende (locally with minor amounts of brannerite and coffinite) as the main ore mineral, accompanied by minor amounts of pyrite, chalcopryrite and galena. A small number of deposits contain elevated concentrations of Co-Ni-Pb-Cu-Au-Ag-Pt in addition to U, and are characterized by development of various sulfides, arsenides and selenides (Robinson, 1955; Beck, 1986). In both cases, the gangue minerals are mainly carbonate (dolomite and calcite), quartz, chlorite, and hematite (Beck, 1986), with or without albite (Kennicott et al., 2015; Liang et al., 2017). The U-dominated deposits of simple mineralogy are distributed throughout the Beaverlodge district and mainly developed in the basement, whereas the U-polymetallic deposits with complex mineralogy are limited in a few small areas and are hosted both by the basement rocks and sedimentary rocks in the Martin Lake Basin (Robinson, 1955; Beck, 1986).

In the Fay – Ace – Verna deposits (the most important ones in the Beaverlodge district), which are distributed along the St. Louis fault (Fig. 1c), the orebodies are developed both in the footwall (Fay deposit,

Fig. 2a) and hanging wall (Verna deposit) of the fault. The mineralization of the Fay and Ace deposits extends over a length of 3000 m along strike and a vertical depth of 1500 m (Beck, 1986; Smith, 1986). The immediate host rocks to the ores can be either granitic rocks or amphibolite – quartzite of the Murmac Bay Group, both having been subjected to strong brittle-ductile deformation and hydrothermal alteration, especially chloritization and albitization. The mineralization appears to be best developed where multiple lithologies rather than solely granites occur. The ore minerals (mainly pitchblende, with minor amounts of brannerite and pyrite) are disseminated in breccias or occur in fractures crosscutting albitized granites (Fig. 3a), together with gangue minerals including quartz, carbonates, hematite, chlorite, and epidote (Beck, 1986). It is remarkable that in addition to granites and amphibolite – quartzite, the Martin Group sedimentary rocks also partly host the mineralization, both within the fault zone and at the unconformity between the Martin Lake Basin and the granitic basement (Figs. 2a, 3b) (Smith, 1986).

In the Gunnar deposit, which is hosted by the 2321 ± 3 Ma (Hartlaub et al., 2007) Gunnar granite near its intrusive contact with Archean orthogneisses (Figs. 1c, 2b; Evoy, 1986; Ashton, 2010), uranium mineralization is closely associated with an albitization zone (Fig. 2c). The albitite, which is characterized by depletion of quartz (Fig. 3c) and was initially termed ‘episyenite’ (Evoy, 1986), is composed of up to 90% albite and as much as 30% carbonate filling vugs and in veins, along with minor chlorite, specular hematite and rutile. The main orebody is hosted in a breccia pipe with a maximum diameter of 150 m and a plunge length of 700 m within the albitite, and the mineralization is characterized by pitchblende and uranophane with chalcopryrite, pyrite, galena, quartz, chlorite, and kaolinite (Beck, 1986).

The vein-style mineralization is widely developed in the basement rocks across the Beaverlodge district, mainly hosted in granites and leucogranites, including Dubyna, Hab, Eagle Shaft, Spur, Intermediate Zone, Camdeck, 21 Zone, 11 Zone and National Exploration (Fig. 1c), and some in amphibolite – quartzite and other metamorphic rocks of the Murmac Bay Group, including Bolger, Eagle-Ace, Lorado and Nicholson (Fig. 1c), as well as in mixed lithologies of orthogneiss, amphibolite and leucogranite (46 Zone, Leonard and Cayzor) (Fig. 1c). There are typically multiple generations of veins within a deposit, and most of them are subvertical, e.g., Dubyna (Figs. 2c, 3d) and Bolger (Fig. 3e). The mineralogy of the veins varies with generations and from one deposit to another, but most of the veins are dominated by quartz and carbonate (dolomite and/or calcite, with both Fe-poor and Fe-rich varieties), with variable amounts of chlorite, albite and hematite (Liang et al., 2017). Pitchblende (uraninite) is the main ore mineral, with minor amounts of pyrite and chalcopryrite. No obvious difference between uraniferous and barren veins can be discerned, but it is notable that the majority of the uraniferous veins contain dolomite (Liang et al., 2017). Although replacement albitization appears to predate uranium mineralization (Fig. 3a, c, d), many of the ore-bearing veins also contain albite (Kennicott et al., 2015; Liang et al., 2017). Hematite is also developed both before mineralization (associated with replacement albitization) and during mineralization (Kennicott et al., 2015; Liang et al., 2017).

Minor amounts of vein-style mineralization are also developed in the basal conglomerate of the Martin Group at many localities around the perimeter of the Martin Lake Basin as well as within the basin, e.g., the Martin Lake and Pitch-Ore deposits, which are located along the southwestern extension of the St. Louis fault (Fig. 1c). The mineralization occurs as veins in fractures within mafic flows, but these fractures become barren when continuing into arkose beds (Fig. 2d) (Smith, 1986). The veins are mainly made of calcite and contain pitchblende, specularite (Fig. 3f), and minor amounts of chalcopryrite, selenides of lead and copper and native copper (Beck, 1986). The ore-bearing calcite veins crosscut albite veins and are cut by barren calcite veins (Fig. 3f). No significant difference is discernable between ore-bearing veins in the basement rocks and those crosscutting the rocks

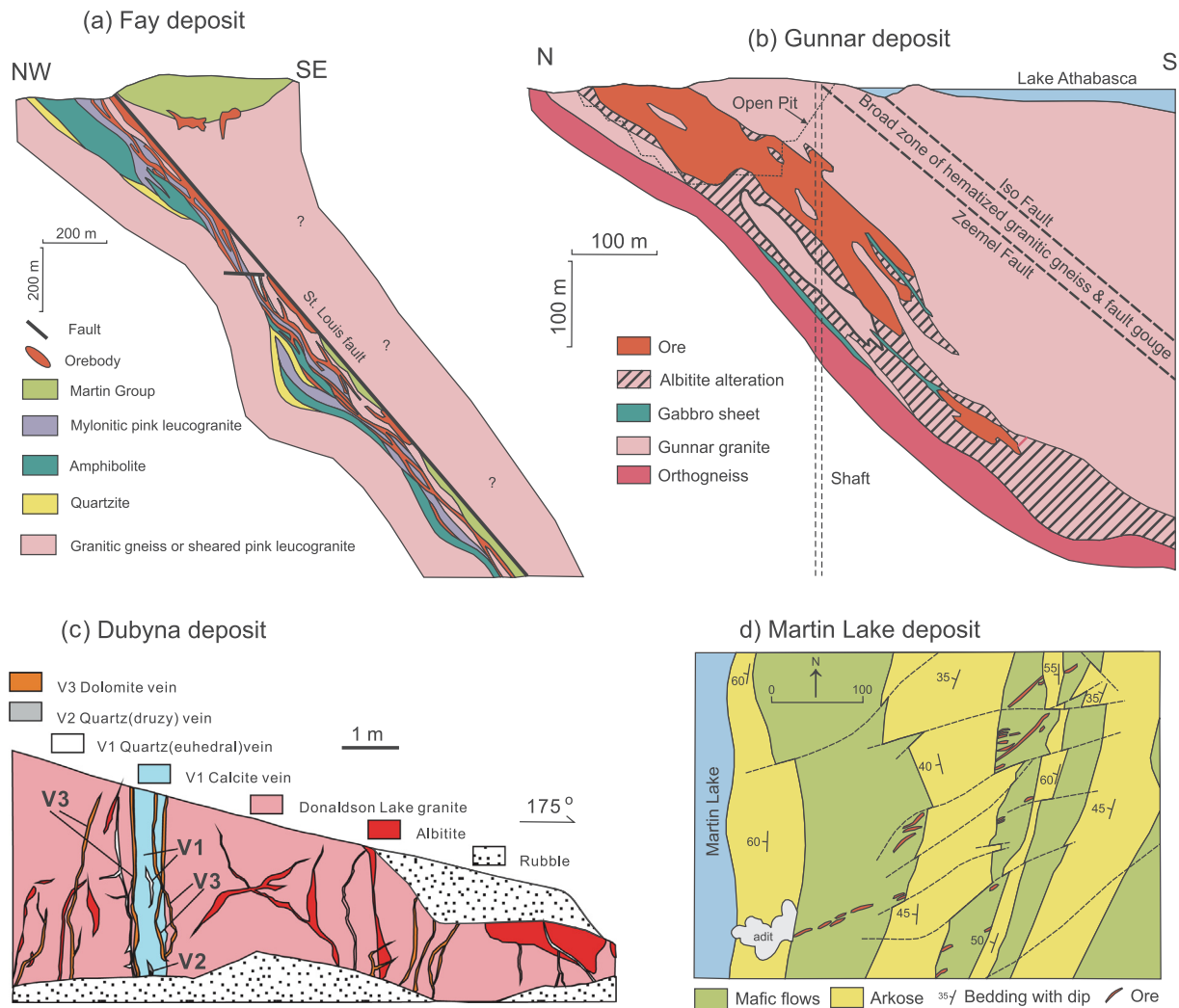


Fig. 2. Geological maps and/or cross sections of uranium deposits from the Beaverlodge district. a) Fay deposit (modified from Smith, 1986); b) Gunnar deposit (modified from Evoy, 1986); c) Dubyna deposit (portion of the open pit; after Liang et al., 2017); d) Martin Lake deposit (modified from Smith, 1986).

within the Martin Lake Basin (Kennicott et al., 2015; Liang et al., 2017).

2.3. Mineralization ages

Various efforts have been made to determine the ages of the uranium mineralization in the Beaverlodge district in a number of previous studies (Robinson, 1955; Koepfel, 1968; Beck, 1969; Tremblay, 1972; Dieng et al., 2013, 2015 and references therein). Based on the occurrences of uranium mineralization and their relationships with the host rocks, the uranium mineralization has been generally divided into two categories, i.e., syngenetic (mineralization formed at the same time as the host rocks) and epigenetic (mineralization that occurred after the host rocks), and it has been generally agreed that the epigenetic mineralization is much more important than the syngenetic one (Robinson, 1955; Koepfel, 1968; Beck, 1969; Tremblay, 1972). However, the ages of each category of mineralization vary significantly for different authors. Thus, Robinson (1955) estimated the syngenetic mineralization to be between ca. 1700 and 1800 Ma based on U-Pb isotopic ages of monazite from the host rocks, and Koepfel (1968) recognized two groups of syngenetic mineralization ages at ca. 2200 Ma and 1930 ± 40 Ma, based on U-Pb isotopic dating of uraninite in the ores and monazite and zircon in the host rocks, whereas Beck (1969) proposed the syngenetic mineralization to be mainly in the range of 1900 to 1850 Ma. Variable U-Pb isotopic ages have also been obtained for pitchblende resulting from epigenetic mineralization, which were

generally interpreted as an initial mineralization followed by multiple remobilization or isotopic resetting events, e.g., ca. 1600 – 1400 Ma initial emplacement followed by ca. 950 – 850 Ma and ca. 350 – 250 Ma resetting events (Robinson, 1955), and 1780 ± 20 Ma initial mineralization followed by 1110 ± 50 Ma, 270 ± 15 Ma and ca. 100 Ma – present resetting events (Koepfel, 1968). Beck (1969) synthesized earlier data to suggest an initial mineralization at ca. 1800 – 1750 Ma followed by multiple periods of undefined remobilization.

A more recent U-Pb isotopic dating of uraninite from various deposits/occurrences in the Beaverlodge district by Dieng et al. (2013, 2015), using laser ablation – high resolution – inductively coupled plasma – mass spectrometry (LA-HR-ICP-MS) technology, yielded a large number of in situ isotopic ages for individual uraninite crystals (Fig. 4). These ages are broadly comparable to those obtained in previous studies (e.g., Robinson, 1955; Koepfel, 1968) (Fig. 4). Based on the new age data and petrographic constraints, Dieng et al. (2013, 2015) suggested six distinct stages (U1 – U6) and settings of epigenetic uranium mineralization, including 2293 ± 17 Ma ‘cataclasite-type’ uraninite (U1), 2289 ± 20 Ma ‘early tensional vein-type’ uraninite (U2), 2321 ± 3 Ma uraninite related to Na metasomatic alteration (U3), 1848 ± 5 Ma ‘breccia-type’ uraninite (U4), 1812 ± 15 Ma ‘volcanic-type’ uraninite (U5), and 1620 ± 4 Ma ‘late vein-type’ uraninite (U6) (Fig. 4). However, it is notable that there is a wide range of ages for each type of uranium mineralization, and there are significant overlaps between different types (Fig. 4). Among the different types of

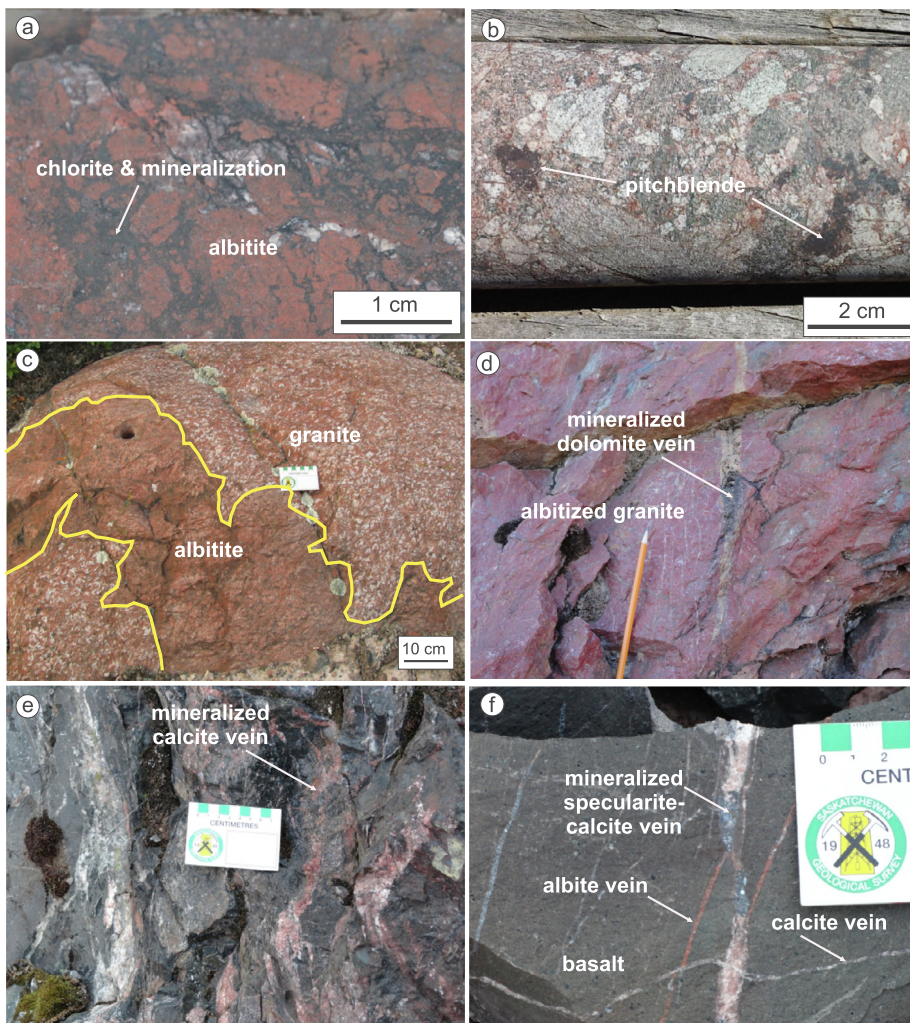


Fig. 3. Photographs showing the characteristics of different styles of uranium mineralization in the Beaverlodge district. a) Breccia-type ore from the Fay deposit; b) Patches of uraninite overprinting conglomerate from the basal part of the Martin Group at the Fay deposit; c) Albitite crosscutting granite at the Gunnar deposit; d) Subvertical dolomite veins (mineralized) crosscutting albitized leucogranite at the Dubyna deposit; e) Subvertical calcite veins (mineralized) developed in amphibolite at the Bolger deposit; f) A calcite – specularite vein (mineralized) crosscutting an offset albitite vein and cut by later calcite veins developed in mafic volcanic rocks at the Martin Lake deposit.

ores, the most important is the breccia-type in terms of tonnage of ore (Tremblay, 1972; Beck, 1986; Dieng et al., 2015); however, the so-called ‘volcanic-type’, which actually represents the vein-type mineralization as indicated in Dieng et al. (2015), is also important because it is the most abundant style of uranium mineralization in the Beaverlodge district (Tremblay, 1972; Beck, 1986; Liang et al., 2017). It is notable that the peak $^{207}\text{Pb}/^{206}\text{Pb}$ ages of the ‘volcanic-type’ ore overlap with those of the breccia-type ore as well as that of the volcanic rocks in the Martin Lake Basin (Fig. 4).

2.4. Ore-forming fluids and P-T conditions

Several studies have been conducted to examine the nature of the ore-forming fluids and the pressure – temperature conditions of uranium mineralization in the Beaverlodge district, using stable isotope, chlorite geothermometry and fluid inclusion techniques (Sassano et al., 1972; Tortosa and Langford, 1986; Rees, 1992; Dieng et al., 2015; Liang et al., 2017). Sassano et al. (1972) suggested that the mineralizing fluids were mainly metamorphic in origin, and incrementally cooled from $\sim 440^\circ$ to $\sim 80^\circ$ C through several paragenetic stages, with surface water involvement in the latest stage. Tortosa and Langford (1986), on the other hand, emphasized that the main phase of uranium mineralization postdated metamorphism, and proposed that the wide range of oxygen isotope values recorded in the carbonates associated with mineralization may be best explained by meteoric water as the main source of the ore-forming fluids. Rees (1992) proposed that basinal fluids may be responsible for uranium mineralization, including U-PGE-

Au mineralization during the deposition of the Martin Group ($100\text{--}200^\circ$ C, 28–36 wt% NaCl eq.) and unconformity-type uranium mineralization during the deposition of the Athabasca Group ($100\text{--}200^\circ$ C, 10–40 wt% NaCl eq.). Dieng et al. (2015), mainly based on H-O-C isotope data of carbonate and chlorite, proposed different fluid sources for different stages of uranium mineralization, including metamorphic fluids ($\sim 300^\circ$ C) for cataclastite-type (U1) and early tensional vein-type (U2) mineralization, magmatic fluids ($\sim 315^\circ$ C) for Na metasomatism-type mineralization (U3), metamorphic fluids ($\sim 330^\circ$ C) for breccia-type mineralization (U4), magmatic fluids ($\sim 315^\circ$ C) for volcanic-type mineralization (U5), and basinal brines ($\sim 235^\circ$ C) for Athabasca-type (U6) mineralization.

Liang et al. (2017) carried out a detailed study of fluid inclusions from various ore veins in the Beaverlodge district, which yielded homogenization temperatures from 78° to 330° C (mainly 100° to 250° C) and salinities from 0.2 to 30.8 wt% NaCl equivalent (Fig. 5a), with a composition system of $\text{H}_2\text{O}\text{--}\text{NaCl}\text{--}\text{CaCl}_2$. Small amounts of CO_2 were detected by mass spectrometry and were below the detection limit of Raman spectroscopy (Liang et al., 2017). The homogenization temperature data are consistent with those estimated from calcite – quartz oxygen isotopic geothermometry (Liang et al., 2017). They also documented extensive evidence for fluid boiling, which, together with low concentrations of volatiles, suggests that fluid pressure was likely lower than 200 bars during at least part of the period of vein formation and mineralization (Liang et al., 2017). Based on the fluid inclusion data and C-O isotopes of carbonates in the veins, it was inferred that the ore-forming fluids for the vein-type mineralization were mainly derived

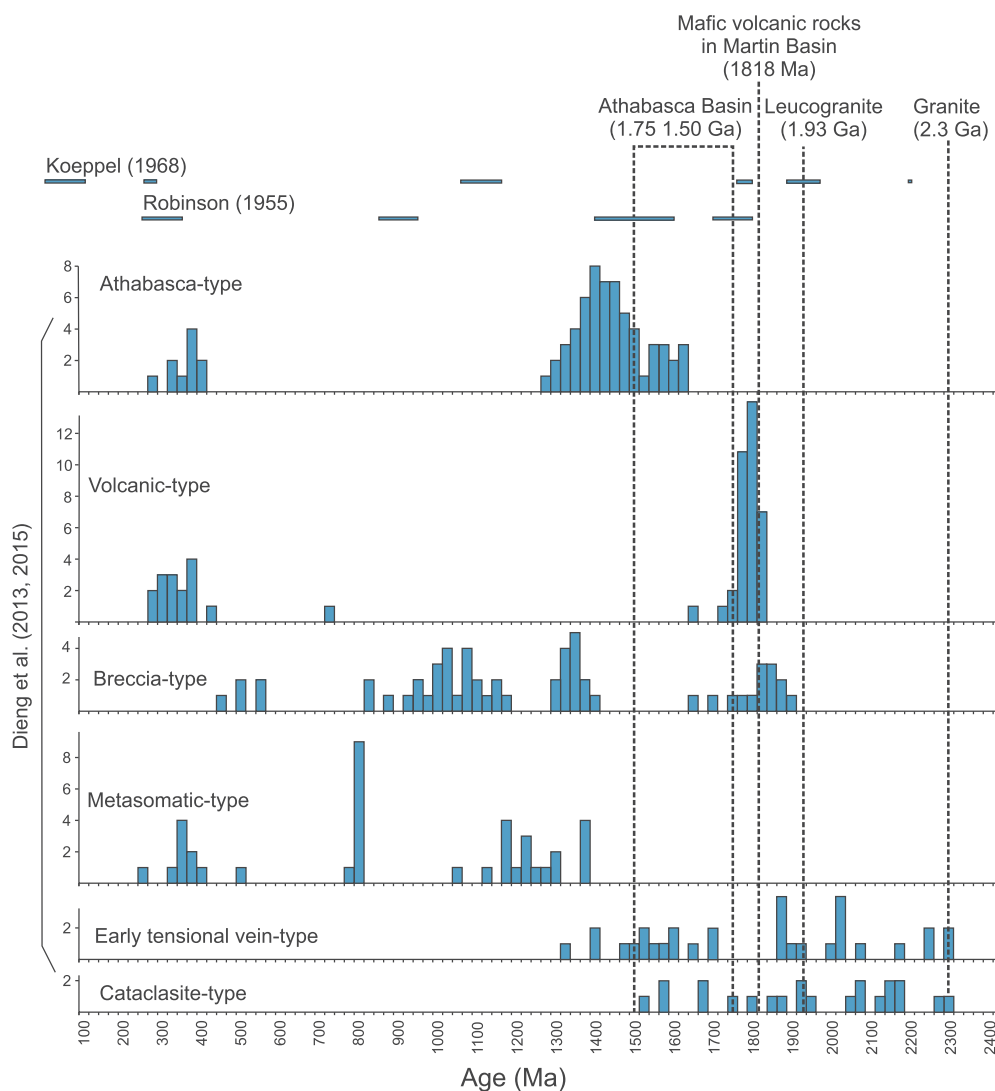


Fig. 4. U-Pb isotopic ages of uraninite from the Beaverlodge uranium district compiled from the data of Dieng et al. (2013, 2015; $^{207}\text{Pb}/^{206}\text{Pb}$ ages), Robinson (1955) and Koeppel (1968). The ages of the host granites and the Martin Lake Basin and Athabasca Basin are illustrated for reference. See text for discussion about the significance of the age data.

from the Martin Lake Basin, although fluids from other sources including residual metamorphic fluids in the basement and meteoric water from the surface may have also been episodically involved (Liang et al., 2017).

Much of the difference between the various studies regarding the sources and thermal conditions of the mineralizing fluids is related to the discrepancy in temperature estimation. The elevated fluid inclusion homogenization temperatures (up to 440 °C) reported by Sassano et al. (1972) were likely due to simultaneous trapping of liquid and vapor phases (i.e., heterogeneous trapping) in a boiling system (Liang et al., 2017). The fluid temperatures calculated from oxygen isotope fractionation between chlorite and carbonate (235 to 330 °C) by Dieng et al. (2015) may also be overestimated, because the chlorite has been affected by late fluids at lower temperatures (Dieng et al., 2015), which tends to increase $\delta^{18}\text{O}$ values of the chlorite, hence decreasing the isotopic difference between chlorite and carbonate and increasing the estimated temperatures. In fact, the chlorite geothermometry yielded significantly lower temperatures (186 to 331 °C for chlorite interpreted to be associated with mineralization, and 111 to 278 °C for chlorite interpreted to be affected by late fluids; Dieng et al., 2015) than those from the isotopic geothermometry. The fluid inclusion homogenization temperatures reported by Rees (1992) (100 to 200 °C) and Liang et al.

(2017) (mainly 100 to 250 °C) are considered to be more representative of the thermal conditions of the ore-forming fluids.

It is important to note that stable isotope data cannot independently determine the source of fluids, because the isotopic fractionation between the parent fluid and the vein minerals depends strongly on temperature. Thus, from similar C-O isotope datasets (Fig. 5b), Dieng et al. (2015) came to the conclusion that the ore-forming fluids were metamorphic or magmatic, whereas Liang et al. (2017) thought they were mainly basinal fluids (Fig. 5c). Furthermore, although the $\delta^{13}\text{C}_{\text{V-PDB}}$ values of the parent fluids overlap with those of magmatic and metamorphic fluids (Fig. 5c), the range (~ -13 to $+1\%$) is much larger than the latter, which is consistent with multiple fluid sources including basinal fluids.

2.5. Mineralization models

Excluding the syngenetic uranium mineralization, which has been considered economically unimportant (Robinson, 1955; Beck, 1969, 1986; Tremblay, 1972), it is generally agreed that the majority of uranium deposits in the Beaverlodge district formed from hydrothermal fluids channelled in faults and fractures. However, the nature of the ore-forming fluids and their relationships to various geologic events in the

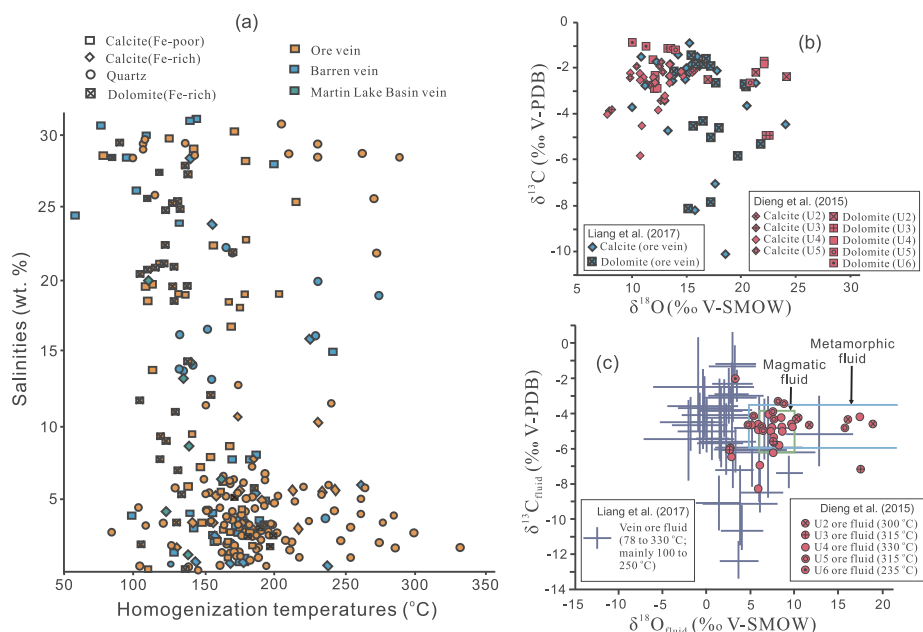


Fig. 5. a) Fluid inclusion homogenization temperature – salinity diagram showing fluid inclusion data from quartz, calcite and dolomite in ore veins, barren veins, and veins within the Martin Lake Basin (modified from Liang et al., 2017); b) $\delta^{18}\text{O}_{\text{V-SMOW}} - \delta^{13}\text{C}_{\text{V-PDB}}$ diagram of carbonates from ore veins (data from Liang et al., 2017, and Dieng et al., 2015); note the overlap between the datasets from the two separate studies; c) $\delta^{18}\text{O}_{\text{V-SMOW}} - \delta^{13}\text{C}_{\text{V-PDB}}$ diagram of fluids calculated from the values of the carbonates; note the difference of between the datasets of Liang et al. (2017) and Dieng et al. (2015), which is mainly due to the difference in the temperatures used in the isotope fractionation calculation.

region, as well as the P-T conditions of mineralization and the mechanisms of ore precipitation, remain contentious.

A major issue is the relative timing of the main phase of mineralization with the development of the Martin Lake Basin. While minor mineralization may have taken place over a wide range of ages overlapping with the ca. 2.3 Ga granite and ca. 1.93 Ga leucogranite (Fig. 4), the dominant styles of mineralization (breccia-type and vein-type) clearly postdate the granites. Dieng et al. (2013, 2015) interpreted the breccia-type mineralization to be pre-Martin Lake Basin and related to metamorphic fluids. However, the fact that Martin Group sedimentary rocks were involved in the deformation associated with the St. Louis fault and overprinted by uranium mineralization (Fig. 2a) suggests that the main phase of uranium mineralization in the Fay – Ace – Verna deposits, the most important ones in the Beaverlodge district, took place after the initial sedimentation of the Martin Lake Basin. Furthermore, based on the observation that the vein-type mineralization in the Martin Lake Basin volcanic rocks is located along the potential southwestward extension of the St. Louis fault (Fig. 1c), it is inferred that the vein-type mineralization, including those developed in the basement rocks, is largely coeval with the breccia-type mineralization, i.e., syn- to post-Martin Lake Basin. This inference is supported by the overlapping ages of ‘volcanic-type’ and ‘breccia-type’ ores with that of the Martin Group volcanic rocks (Fig. 4), and the overall similarity in mineralogy and C-O isotope composition of carbonates between the vein ores and breccia ores (Fig. 5b). The observation that the oldest ages of the breccia-type ore (ca. 1850 Ma, considered to represent the time of breccia-type mineralization by Dieng et al., 2013, 2015) are older than the volcanic rocks (ca. 1820 Ma) may be related to the nature of the $^{207}\text{Pb}/^{206}\text{Pb}$ ages, which could be higher than ages estimated from other methods due to radioactive daughter leakage (Ludwig and Simmons, 1992).

As discussed above, the ore-forming fluids were likely basinal brines derived from the Martin Lake Basin. These oxidizing basinal fluids may have infiltrated the basement, perhaps periodically enhanced by faulting and the suction pump mechanism (Sibson, 1987), and reacted with the basement rocks (especially the ca. 2.3 Ga and 1.9 Ga granites) to acquire large amounts of uranium. However, these basement rocks are also the source rocks for the sediments in the Martin Lake Basin, and it is possible that significant amounts of uranium may have also been derived from sedimentary rocks within the basin, as was suggested for the Athabasca Basin (Chi et al., 2019). Uranium precipitation may have

taken place due to mixing between the uraniferous fluids and fluids containing reducing agents (especially CH_4 and Fe^{2+}) derived from the basement. Fluid-rock interaction and fluid boiling may have also contributed to uranium precipitation (Liang et al., 2017). Although the mineralization is mainly hosted in the basement, many of the deposits are located near the Martin Lake Basin (Figs. 1c, 2a), and thus, in a sense, the uranium mineralization in the Beaverlodge district may be compared to the unconformity-related uranium deposits in the Athabasca Basin, despite their significant differences in vein mineralogy, alteration type, and age (Liang et al., 2017).

3. Granite-related uranium mineralization in South China

3.1. Geological setting

The granite-related uranium deposits in South China are mainly distributed in the Cathaysia Block and the Jiangnan Orogen (Fig. 6a), which are part of the South China Craton or South China Block, well known for its rich endowment of world-class W and Sn deposits related to Mesozoic granites (Mao et al., 2013). The Cathaysia Block was amalgamated with the Yangtze Block to form the South China Block during the Neoproterozoic Jiangnan orogeny (Shu et al., 1994; Charvet et al., 1996), which may have taken place at ca. 1100 – 900 Ma (Grenville orogeny; Li et al., 1999, 2008) or ca. 860 – 820 Ma (Zhou et al., 2009; Zhao and Cawood, 2012; Deng et al., 2019). Much of the Jiangnan Orogen was initially part of the Yangtze Block, which is separated from the Cathaysia Block by the Jiangshan – Shaoxing fault (suture zone) (Fig. 6a). The Yangtze Block consists of Archean to Neoproterozoic rocks, and the Jiangnan Orogen comprises mainly Neoproterozoic rocks, whereas the Cathaysia Block is made of Paleoproterozoic to Neoproterozoic rocks, although detrital zircons of Archean ages have also been widely reported (Zhao and Cawood, 2012). Pre-, syn- and post-orogenic granitic rocks (ca. 1000 to 750 Ma) were well developed in the Jiangnan Orogen (Fig. 6a).

Following the assembly of the Yangtze and Cathaysia blocks, an extensional basin called the Nanhua Basin was developed over much of the Jiangnan Orogen and a significant portion of the Cathaysia Block in early Neoproterozoic time (the Banxi Group and equivalents; < 830 Ma), with the tectonic setting being variably interpreted as plume-related rifting (Wang and Li, 2003), back-arc spreading (Zheng et al., 2008), and post-collisional extension associated with

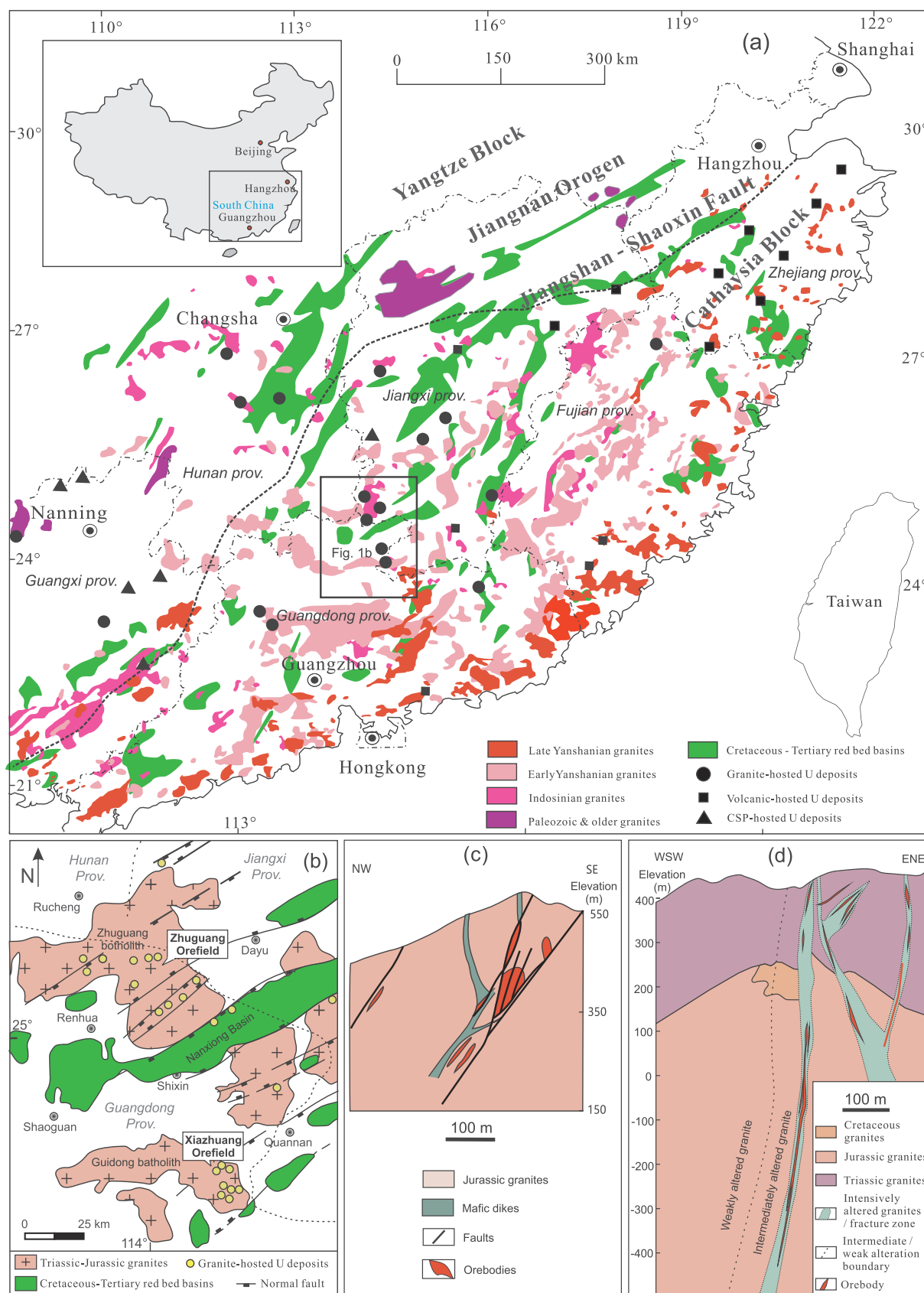


Fig. 6. a) A simplified geological map of South China showing the distribution of granites of different ages, Cretaceous – Tertiary red bed basins, and major types of uranium deposits (modified from Zhou et al., 2006; Hu et al., 2008; Zhang et al., 2019); b) A simplified geological map of the Xiashuang and Zhuguang uranium orefields in northern Guangdong Province, showing the distribution of granites, Cretaceous – Tertiary red bed basins, and uranium deposits (modified from Luo et al., 2015; Bonnetti et al., 2018); c) A cross section of the Xiawang uranium deposit in the Xiashuang orefield (modified from Li et al., 2011); d) A cross section of the Mianhuakeng uranium deposit in the Zhuguang orefield (modified from Zhang et al., 2016).

mantle upwelling (Zhao and Cawood, 2012). Sedimentation in the Nanhua Basin continued through the remaining of the Neoproterozoic and early Paleozoic periods until the Caledonian orogeny, which created a regional unconformity between Early Paleozoic and older rocks and overlying Devonian and younger rocks (Charvet et al., 2010). The Caledonian orogeny is characterized by the development of generally NE-trending folds and thrust faults and variable degrees of regional metamorphism (peaking at 440–430 Ma) as well as granitic intrusions, and has been interpreted as an intracontinental orogeny related to the underthrusting of the southern part of the Cathaysia Block beneath its northern part (Charvet et al., 2010).

After a relatively stable tectonic regime from Devonian to middle Triassic time, characterized by shallow marine carbonate and clastic sedimentation, South China was subjected to another tectonic event called the Indosinian orogeny in the late Triassic Period. The Indosinian orogeny has been variably attributed to the collision of the South China Block with the Indochina Block (associated with the closure of the Paleo-Tethys Ocean; Faure et al., 2014) and with the North China Block (associated with the closure of the Paleo-Tethys Qinling Ocean; Meng and Zhang, 2000) in late Triassic time, and to flat-slab subduction of the Paleo-Pacific plate underneath the South China Block, which started as early as late Early Permian time (Li et al., 2006; Li and Li, 2007). The Indosinian orogeny in South China is manifested by a regional unconformity between Upper Triassic strata and various older rocks, development of a series of folds and thrust faults in Devonian to middle Triassic strata (Guo, 1998), and emplacement of granitic intrusions (mostly from 240 to 210 Ma, and some from 280 to 240 Ma; Li and Li, 2007). Carter and Cliff (2008) emphasized that the Indosinian orogeny in South China is not a mountain building tectonic event resulting from proximal plate collisions, but rather a thermotectonic reactivation event caused by more distal tectonic activity.

From late Jurassic to Cretaceous time, South China experienced another episode of intensive intracontinental orogeny called the Yanshanian orogeny (Wong, 1927). This orogeny and the Indosinian orogeny were collectively considered as tectonic reactivations after a relatively stable platform regime (Chen, 1956), and it is believed to be responsible for the “destruction of North China craton” or “reworking of South China continent” (Zhu et al., 2012). The Yanshanian orogeny is manifested by a number of unconformities within Jurassic and Cretaceous intracontinental basins, folding and faulting of rocks within these basins and older rocks, and development of voluminous terrestrial volcanic rocks and granitic intrusions (Fig. 6a). The granitic rocks, including I-, S- and A-types, have been generally divided into Early Yanshanian (Jurassic, > 145 Ma) and Late Yanshanian (Cretaceous, < 145 Ma) (Zhou et al., 2006; Mao et al., 2013), or an early period (175 to 120 Ma) and a later period (110 to 75 Ma) (Li et al., 2014). The Yanshanian orogeny is generally attributed to subduction of the paleo-Pacific plate underneath the eastern Asian margin, although there are different opinions regarding the timing, mode and evolution of the subduction (Zhou et al., 2006; Li and Li, 2007; Sun et al., 2007). Nevertheless, as summarized in Xu et al. (2017), it is generally agreed that during the Mesozoic, the eastern part of China, including South China, went through a series of evolving tectonic settings, from the ca. 230–210 Ma collisional orogeny (Indosinian orogeny), through the ca. 180–160 Ma subduction of the paleo-Pacific plate beneath the Eurasian continental margin, to the ca. 150–80 Ma lithospheric thinning and delamination resulting from plate rollback and foundering. During the last period, the overall extensional setting led to the development of a basin-and-range-like province in South China characterized by bimodal magmatism and a large number of NE-SW trending basins (Li and Li, 2007). These extensional basins are characterized by the development of large volumes of red beds, which continued into early Tertiary time (Fig. 6a).

3.2. Geological characteristics of granite-related uranium mineralization

The uranium deposits in South China have been classified into four main types, i.e., granite-hosted, volcanic-hosted, carbonaceous-siliceous-pelitic sedimentary rock-hosted, and sandstone-hosted, of which the former two are the most important (Du and Wang, 1984; Huang et al., 1994; Hu et al., 2008; Dahlkamp, 2009; Zhang et al., 2019). It has been argued by many authors that the different types of deposits may be genetically related (Du and Wang, 1984; Wang et al., 2002; Hu et al., 2008; Chi and Zhou, 2012; Zhang et al., 2019) and therefore, many of these deposits may be classified as granite-related according to the criteria of the IAEA (2018). However, there are still controversies regarding how these deposits may be related to each other (e.g., Hu et al., 2008; Zhang et al., 2019), and classifying them all as granite-related can be misleading. Therefore, in this paper we mainly limit our study to the uranium deposits hosted within granite intrusions.

At regional scale, it has been noticed that many of the granite-hosted uranium deposits in South China are spatially associated with the Cretaceous – Tertiary red bed basins (Zhang, 1989; Wang et al., 2002; Zhang et al., 2019) (Fig. 6a). At district scale, it has been shown that although most granite-hosted uranium deposits are not directly overlain by the red bed basins, they are close to each other, as shown by the Xiazhuang and Zhuguang uranium orefields in northern Guangdong Province (Fig. 6b) (Hu et al., 2008; Luo et al., 2015; Bonnetti et al., 2018; Zhang et al., 2019). It is also noticeable that many of the granite-hosted uranium deposits are located close to regional NE-trending normal faults, both at regional and district scales (Deng et al., 2003; Hu et al., 2008; Zhang et al., 2019). Minor amounts of uranium mineralization also occur within some of the red bed basins immediately adjacent to granite-hosted uranium districts (Xia et al., 2016).

The most important granite-hosted uranium deposits in South China are distributed in the Nanling Range, mainly in Guangdong and Jiangxi provinces (Fig. 6a). They are particularly well developed in the Xiazhuang and Zhuguang orefields in northern Guangdong (Fig. 6b), which contain about 37,000 t of identified U resources (NEA-OECD, 2018) with grades generally from 0.1 to 0.5% U (Dahlkamp, 2009; Luo et al., 2015; Bonnetti et al., 2018). In the Xiazhuang orefield, fifteen uranium deposits and a number of uranium occurrences are hosted by the Guidong batholith, which is composed of Triassic (237–220 Ma) and Jurassic (189–151) biotite granite, two-mica granite and muscovite granite that are cut by numerous Jurassic to Cretaceous mafic dikes (Hu et al., 2008; Dahlkamp, 2009; Luo et al., 2015; Bonnetti et al., 2018). The Guidong batholith is located about 30 km south of the Nanxiong Basin and is close to several other Cretaceous – Tertiary basins (Fig. 6b). The orebodies are controlled by ENE-WSW and NE-SW trending steep faults cutting through the granites and are close to mafic dikes (Hu et al., 2008; Dahlkamp, 2009; Li et al., 2011; Luo et al., 2015; Bonnetti et al., 2018), as seen in the Xiwang deposit (Fig. 6c). In the Zhuguang orefield, there are eighteen uranium deposits and a number of uranium occurrences hosted within the Zhuguang batholith, which consists mainly of Triassic (239–226 Ma) and Jurassic (170–159) biotite granite and two-mica granite, with minor amounts of Cretaceous granites (Zhang et al., 2016, 2017; Bonnetti et al., 2018). The Zhuguang batholith is cut by a number of Cretaceous mafic dikes, and is adjacent to the Nanxiong Basin and several other Cretaceous – Tertiary red bed basins; two uranium deposits occur within the Nanxiong Basin near the basin – granite contact (Fig. 6b). The orebodies are mainly distributed along subvertical ENE-WSW, NE-SW and near N-S trending regional faults (Dahlkamp, 2009; Zhang et al., 2016, 2017, 2019), and are characterized by a great vertical extent up to > 800 m, as typified by the Mianhuakeng deposit (Fig. 6d).

The mineralization occurs both in veins and alteration halos in, or close to, fracture zones within granites, which are commonly brecciated (Dahlkamp, 2009; Zhang et al., 2016, 2017, 2019; Bonnetti et al., 2018). The veins are typically composed of quartz, calcite, fluorite, hematite, pitchblende (with minor coffinite) and sulfides (mainly

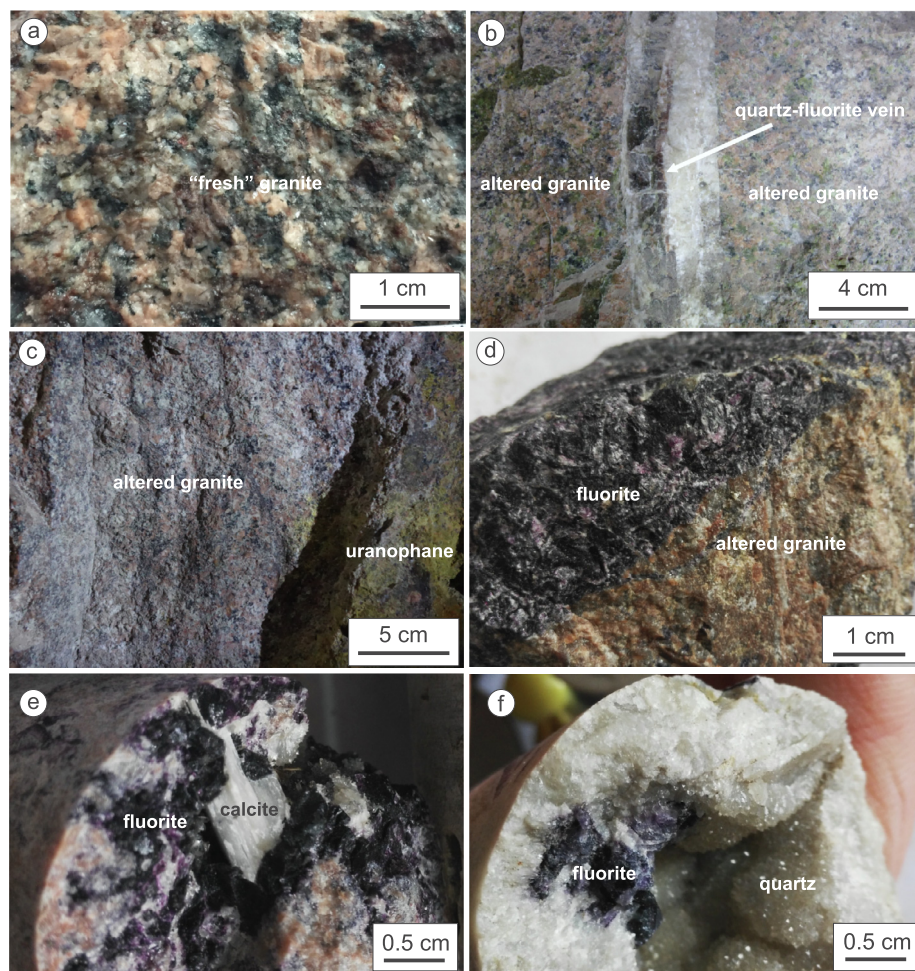


Fig. 7. Photographs of ores and host rocks of the Mianhuakeng uranium deposit showing characteristics of typical granite-hosted uranium deposits in South China. a) Relatively 'fresh' granite away from mineralization; b) A mineralized quartz-fluorite vein surrounded by alteration halo with characteristic apple green illite; c) Disseminated uranium mineralization (manifested by secondary uranophane) in altered host rocks; d) A mineralized fluorite vein with characteristic blackish – deep purple fluorite; e) Deep purple fluorite associated with calcite filling a fracture; f) Deep purple fluorite associated with drusy quartz filling open space. (For interpretation of the references to color in this figure legend, the reader is referred to the web version of this article.)

pyrite, with minor and variable amounts of galena, sphalerite and chalcocopyrite), and these minerals also occur in the alteration halos (Dahlkamp, 2009; Zhang et al., 2016, 2017, 2019; Bonnetti et al., 2018) (Fig. 7). Both biotite (some of which may be hydrothermal) and chlorite are generally present in the weakly altered host granites away from the mineralized zones (Figs. 6d, 7a), but the dominant alteration minerals in the intensively altered granites are illite, which has a characteristic apple green color (Fig. 7b), K-feldspar and hematite (Fig. 7c). The fluorite associated with mineralization has a deep purple color (appearing black in hand samples; Fig. 7d), and is also associated with calcite (Fig. 7e) and quartz (Fig. 7f) with typical open space-filling structures and textures. The uranium mineralization within the basin is controlled by subsidiary fractures of regional extensional faults bounding the basin and granitic intrusions, occurring as veinlets and disseminations of pitchblende and associated sulfides, quartz, calcite and fluorite in gravelly sandstones (Xia et al., 2016). It is remarkable that the mineral assemblages associated with uranium mineralization in the basin are similar to those within the granites.

3.3. Mineralization ages

It has been noticed for a long time that the uranium mineralization of the granite-hosted uranium deposits in South China appears to be much younger than the host granites, mainly based on whole-rock U-Pb isotopic dating (Du and Wang, 1984; Zhang, 1989; Wang et al., 2002). This has been further confirmed in recent years by new geochronological data obtained using in situ analytical techniques such as SIMS and LA-ICP-MS as well as Sm-Nd dating of uraninite and fluorite, as summarized by Hu et al. (2008) and Zhang et al. (2019) and detailed in

Fig. 8. The majority of the granites that host the uranium mineralization are of Early Yanshanian (Jurassic) age (180–142 Ma), and to a lesser extent of Indosinian (Triassic) age (251–205 Ma) (Fig. 6a), while the majority of the reported mineralization ages are Cretaceous and Early Tertiary, especially from ca. 100 to 50 Ma (Fig. 8). Thus, there is an apparent gap of > 40 Ma between uranium mineralization and the host granites for most of the granite-hosted uranium deposits in South China, although minor amounts of mineralization with ages similar to those of the host granites have been found in the Xiazhuang and Zhuguang orefields (Fig. 6b) (Bonnetti et al., 2018). On the other hand, it is notable that the majority of the reported uranium mineralization ages overlap with those of mafic dikes (148 to 46 Ma; Hu et al., 2008), and especially with the Cretaceous – Tertiary red bed basins, which were mainly developed from Late Cretaceous to Paleogene (101 to 23 Ma) (Deng et al., 2003).

3.4. Ore-forming fluids and P-T conditions

A number of fluid inclusion studies have been conducted for the granite-hosted uranium deposits in South China (Fig. 9a and references therein). The host minerals of the fluid inclusions studied include pre-, syn- and post-ore quartz, fluorite and calcite (Fig. 9a). The homogenization temperatures (T_h) of the fluid inclusions range mainly from ~100 to ~300 °C, with a few in the range of 300 to 400 °C (Fig. 9a). There is no systematic difference in T_h between pre-ore and syn-ore minerals, but the T_h values of fluid inclusions in the post-ore minerals are mostly in the lower range, mainly from ~100 to ~200 °C (Fig. 9a). The salinities calculated from ice-melting temperatures of fluid inclusions mainly range from ~1 to ~10 wt% NaCl equivalent, with the

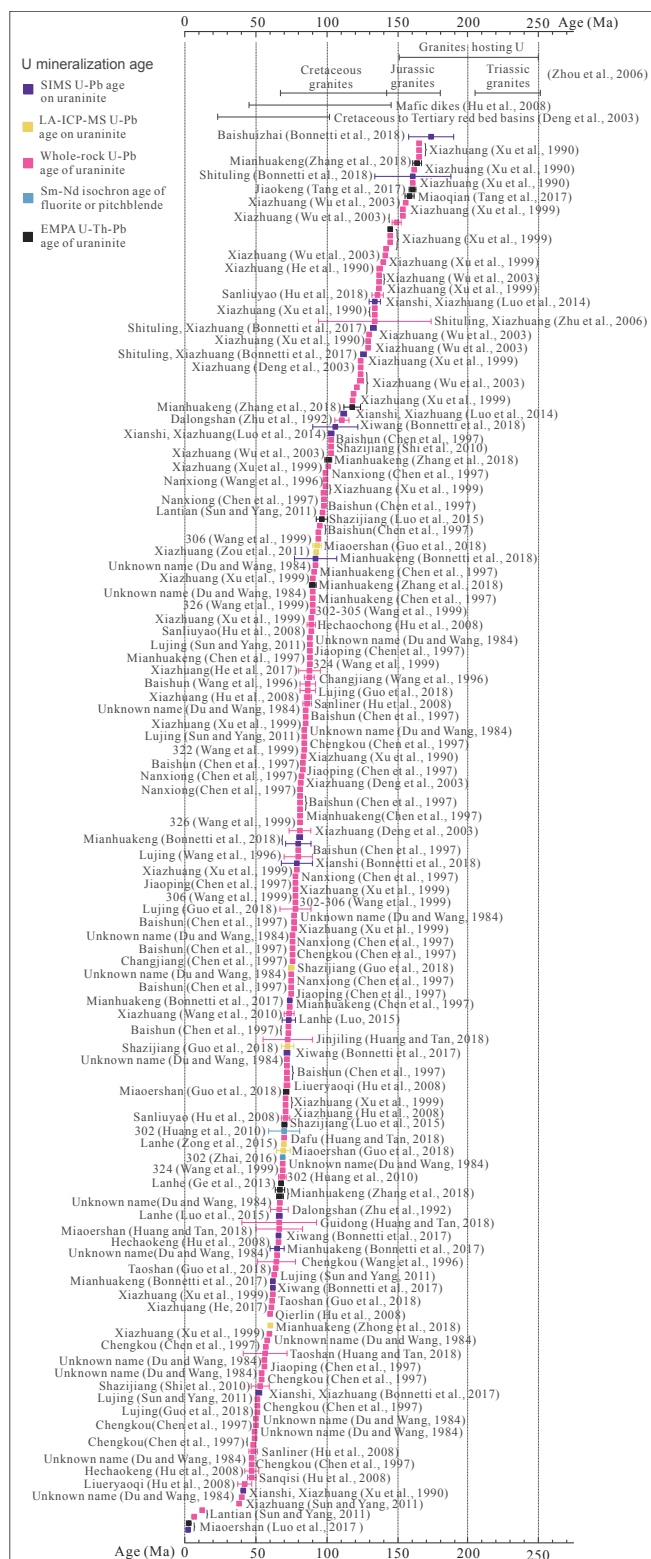


Fig. 8. Compilation of isotopic ages of uranium mineralization in South China (data sources shown in the figure are listed in the appendix).

exception of one deposit having an average salinity of ~15 wt% NaCl equivalent (Fig. 9a). No systematic difference in fluid salinity is discernable between pre-, syn- and post-ore minerals (Fig. 9a). CO₂-bearing fluid inclusions have been reported in many of the granite-hosted uranium deposits, and evidence for fluid boiling or immiscibility have been documented (Hu et al., 2008; Zhang et al., 2016, 2017). CH₄,

H₂ and O₂ were also detected by Raman spectroscopy in some fluid inclusions (Zhang et al., 2016, 2017). Various fluid pressures have been estimated from fluid inclusion studies, varying from 500 to 800 bar (Shen et al., 1988; Min et al., 2005), 1000 – 1100 bar (Zhang et al., 2017), to 1590 – 1790 bar (Wang et al., 1999). However, it is worth noting that all these pressure values were calculated from CO₂-bearing fluid inclusions, and it has been noted that most of these inclusions were developed in the early (mainly pre-ore) hydrothermal stage (Hu et al., 2008). Therefore, the elevated fluid pressures reported in the literature may not represent the fluid pressure regime during the main phase of uranium mineralization.

The isotopic compositions of the fluids involved in mineralization in the granite-hosted uranium deposits in South China have also been examined in a number of studies and summarized in Hu et al. (2008) and Zhang et al. (2019). The $\delta^{13}\text{C}_{\text{V-PDB}}$ values of calcite associated with uranium mineralization range from –10 to –4‰ (Fig. 9b), which are comparable to those of mantle-derived carbon (Hu et al., 2008). The $\delta^{18}\text{O}_{\text{V-SMOW}}$ and $\delta \text{D}_{\text{V-SMOW}}$ values of the mineralizing fluids, estimated from isotopic analysis of fluid inclusions (for H isotopes) and their host minerals (for O isotopes, calculated with estimated temperatures from fluid inclusion studies), mostly fall in the area between the meteoric water line and the fields of magmatic and metamorphic waters in the $\delta^{18}\text{O}_{\text{V-SMOW}} - \delta \text{D}_{\text{V-SMOW}}$ diagram (Fig. 9c; Zhang et al., 2019).

3.5. Mineralization models

The observation that the majority of isotopic ages of uranium mineralization of the granite-hosted uranium deposits in South China are > 40 Ma younger than their host granites (Fig. 8), suggests that the principal uranium mineralization events for most of these deposits are unrelated to the magmatic hydrothermal fluids released from the host granites. Although it cannot be ruled out that the actual mineralization ages are older than the isotopic ages due to potential resetting of the U-Pb isotopic system of uraninite, and indeed some isotopic ages are similar to those of the host granites and suggest an earlier mineralization event of magmatic-hydrothermal nature (Bonnetti et al., 2018), it is likely that the main phase of uranium mineralization took place significantly later than the emplacement of the hosting granites. Thus, the nature of the ore-forming fluids becomes the focus of debate between different genetic models. Geological observations clearly indicate that the granite-hosted uranium deposits in South China are controlled by faults and fractures, and it is generally understood that this is due to the fact that the fracture zones have relatively high permeabilities and are favorable for fluid flow. However, there are different opinions about the sources of the ore-forming fluids and metals.

Regarding the fluid sources, many authors suggest that the ore-forming fluids were originally meteoric water percolating from the surface, which acquired heat during their circulation at depth and became hydrothermal fluids (Du and Wang, 1984; Zhang et al., 2019). Zhang et al. (2019) emphasized that the meteoric water was first accumulated in the Cretaceous – Tertiary red bed basins and then infiltrated into the basement, and so the ore-forming fluids are actually basal fluids. As such, the Mesozoic uranium deposits in South China have been considered comparable to the Proterozoic unconformity-related uranium deposits (Wang et al., 2002; Zhang et al., 2019). On the other hand, Hu et al. (2008), based on the observation of CO₂-bearing fluid inclusions in the uranium deposits, the similarities of carbon isotopes of the hydrothermal calcite with those of mantle carbon, and the recognition that the uranium mineralization is temporally and spatially associated with mafic dikes, proposed that mantle-derived CO₂ contributed to the mineralizing fluids. Hu et al. (2008) suggested that the addition of CO₂ to the ore-forming fluids increased the capacity of the fluids to leach uranium from the source rocks.

As to the sources of uranium, it has been noticed that many of the Mesozoic granitic and volcanic rocks and Proterozoic to Cambrian sedimentary and metamorphic rocks in South China contain elevated

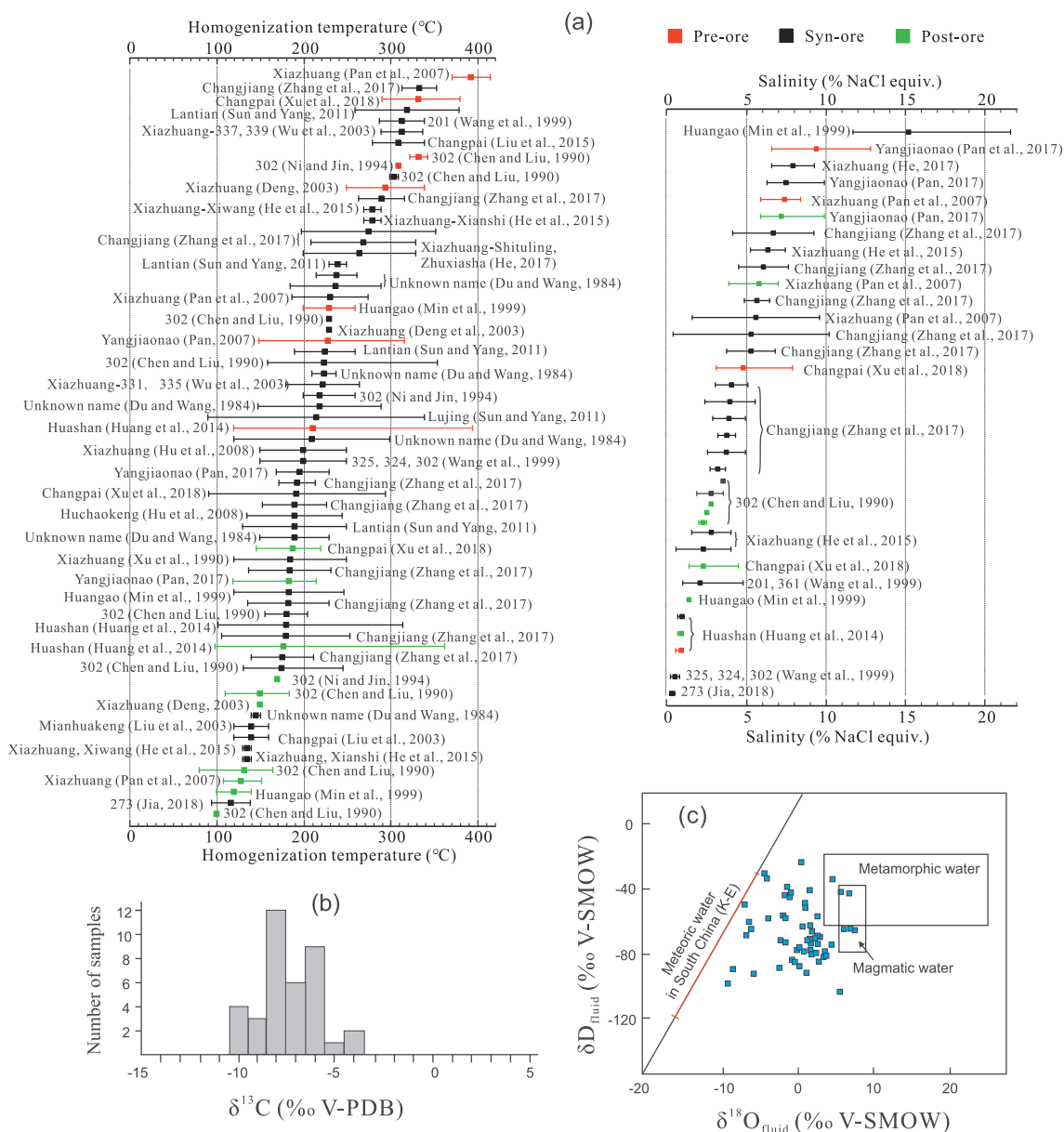


Fig. 9. a) Ranges of homogenization temperatures and salinities of fluid inclusions from granite-related uranium deposits in South China (data sources shown in the figure are listed in the appendix); b) Histogram of carbon isotopic data of calcite associated with granite-related uranium mineralization in South China (modified from Hu et al., 2008); c) Oxygen and hydrogen isotope data of fluids associated with granite-related uranium mineralization in South China (modified from Zhang et al., 2019).

concentrations of uranium from 7 to 39 ppm (see summaries in Hu et al., 2008, Zhang et al., 2019), and may be the ultimate sources of uranium for a variety of uranium mineralization types, including the granite-hosted ones. However, it is uncertain whether uranium was extracted from the source rocks on the surface during chemical weathering (Wang et al., 2002) and within the red bed basins during subsequent sedimentation – diagenetic processes (Zhang et al., 2019), or mainly in the basement (Hu et al., 2008). The possibility that both the sediments in the basins and the basement rocks had contributed to the uranium in the ore-forming fluids cannot be ruled out.

Based on the common presence of calcite and fluorite in the uranium deposits, and the generally low salinities of the ore-forming fluids, it is believed that uranium was mainly transported as uranyl carbonate and uranyl fluoride complexes (Hu et al., 2008; Zhang et al., 2019). Thus, carbonate and fluorite precipitation in the veins and alteration halos, as well as fluid immiscibility and related CO_2 degassing, may be the most direct cause of uranium precipitation (Hu et al., 2008;

Zhang et al., 2017, 2019). Fe^{2+} originally in biotite may have been a major reducing agent for reducing U^{6+} to U^{4+} , as reflected by alteration of biotite and precipitation of hematite accompanying uranium mineralization. However, the presence of CH_4 in the fluid inclusions and development of sulfides in the ores, especially toward the later stage of mineralization (Zhang et al., 2017), suggest that mixing of the uranium-bearing, oxidizing fluid with a reducing fluid may have also contributed to uranium precipitation.

4. Discussion

As mentioned in the introduction, granitoids similar to those in the Beaverlodge district and South China are well developed in many places in the world, but uranium mineralization appears to be preferably concentrated in certain regions, which led to the question of why these regions are particularly favorable for uranium mineralization. We tackle this question through comparison of the uranium mineralization

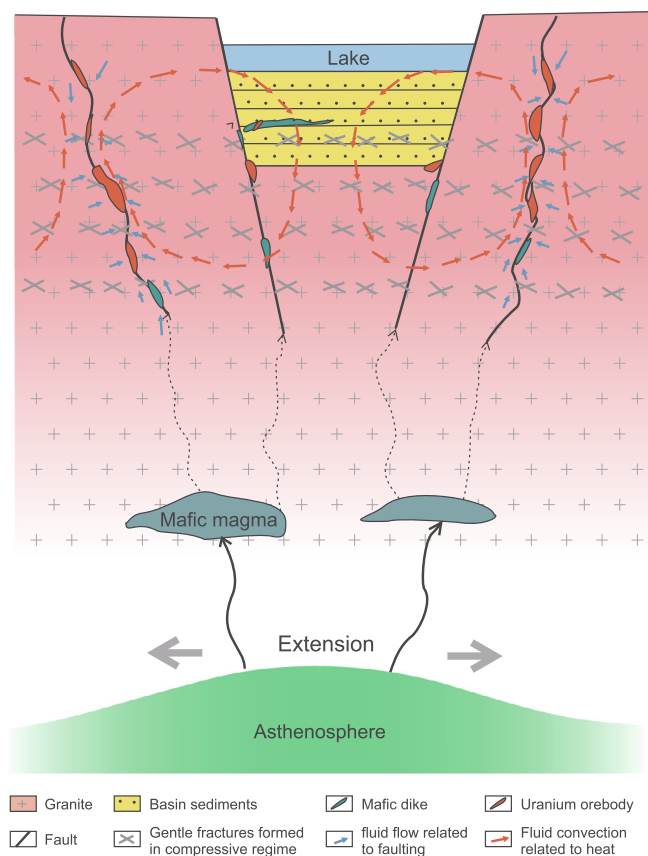


Fig. 10. A generalized mineralization model showing the common controlling factors and processes related to uranium mineralization in the Beaverlodge district and South China (not to scale). The model emphasizes the coupling of shallow (extensional red bed basin) and deep-seated (asthenosphere upwelling and related extensional faulting and magmatism) as the primary controls of the uranium mineralization.

in the Beaverlodge district with the granite-related uranium mineralization in South China. This is done by summarizing the global similarities and differences of the two mineralization systems, and analyzing the common factors that are favorable for mineralization despite the differences in time and local geologic environment. The mechanisms providing the geological control on mineralization, or the mineralization models (Fig. 10), are then discussed.

Obviously, the Beaverlodge district is a much smaller area than South China, but it should be noted that Beaverlodge is just part of an extensive region within the Churchill Province that experienced a similar tectonic history, and uranium mineralization similar to those in Beaverlodge, e.g., the Lac Cinquante uranium deposit hosted in basement rocks at the approximate unconformity of the Baker Lake Group (Martin Group correlative) (Bridge et al., 2013), is developed in the Baker Lake area near the Thelon Basin (Fig. 1a). On the other hand, granite-hosted uranium deposits are not evenly distributed all over South China, but are rather concentrated in certain districts such as the Zhuguang and Xiazhuang orefields (Fig. 6). It should also be borne in mind that the degree of mapping and exploration in northern Canada is relatively low compared to South China, implying that more Beaverlodge-type uranium deposits may remain to be discovered.

The most significant similarities between the uranium mineralization systems in Beaverlodge and South China can be summarized as follow. 1) Both areas are characterized by abundant granitoid rocks that are relatively enriched in uranium, although of greatly different ages (Archean to Paleoproterozoic versus mainly Mesozoic); 2) The mineralization is much younger than the host granites (or granites adjacent to mineralization); 3) The uranium deposits are spatially close to red bed

basins that were developed broadly in the same period of time as the mineralization; some of the mineralization is developed close to the unconformity or within the basin; 4) There was mafic magmatism, manifested as volcanic rocks and dikes, taking place in the same time period as the mineralization; 5) The mineralization is controlled by steep faults or fracture zones with extensional features, some of which were originally formed in compressive or transpressive environments, in accordance with the switch in stress regime from compressive or transpressive to extensional; 6) The mineralization styles include veins and disseminations in breccias and altered wall rocks; 7) The main ore mineral is uraninite or pitchblende, and the main gangue minerals in the veins are mainly quartz and calcite; 8) Alteration halos are developed around the veins, and commonly contain quartz, carbonates, and hematite; 9) Fluid inclusion homogenization temperatures mainly range from 100 to 300 °C, and there is evidence for fluid boiling or immiscibility; and 10) Oxygen and hydrogen isotope compositions of the ore-forming fluids are situated between fields of meteoric water and magmatic – metamorphic fluids, and carbon isotope compositions ($\delta^{13}\text{C}_{\text{V-PDB}}$) are negative and overlap with those of mantle-derived carbon.

The main differences between the mineralization systems in the two areas include the following. 1) Fluorite is more common and abundant in the South China veins than the Beaverlodge ones, whereas albitite is the opposite; 2) Illite is well developed in most of the alteration halos surrounding the South China veins, and it is rarely developed in Beaverlodge; 3) CO_2 is commonly detected in the South China system (especially in the early stage or pre-ore minerals), whereas it is of low concentration in the Beaverlodge ores; 4) The salinities of the ore-forming fluids in South China are mostly lower than 10 wt% (many are lower than 5 wt%) NaCl equivalent and the fluid system may be approximated by $\text{H}_2\text{O}-\text{NaCl} \pm \text{CO}_2$, whereas those in the Beaverlodge district range from near-zero to ~30 wt% (many are > 10 wt%) NaCl equivalent and the fluid system may be represented by $\text{H}_2\text{O}-\text{NaCl}-\text{CaCl}_2$. These differences may be attributed to specific environments and processes in the respective areas. For example, the degree of evaporation may be higher in the Martin Lake Basin in the Beaverlodge district than in the Cretaceous – Tertiary red bed basins in South China, resulting in higher salinities in the basinal fluids in the former than in the latter.

The similarities of the granite-related uranium mineralization systems in Beaverlodge and South China have important implications for the controlling factors of mineralization. The fact that the mineralization significantly postdates the host granites in both areas indicates that the ore-forming fluids could not have been magmatic-hydrothermal fluids derived directly from these granites. Yet, the close spatial relationship between the uranium mineralization and the granites suggests that they are genetically related. Because many of the host granites have relatively elevated concentrations of uranium, it may be assumed that these granites acted as the main source of uranium for the mineralization. However, primary granitic rocks are generally of low permeabilities, and thus it is difficult to extract uranium if they are intact. Thus, brittle faults and fracture zones cutting through the granites, including those that evolved from precursor ductile deformation zones (Beaverlodge), become an important factor controlling uranium mineralization. On the other hand, faults and fractures developed in granites are ubiquitous, but most of them are barren. This implies that, in addition to the presence of a uranium source and high-permeability zones in the granites, there must be other factors that control the mineralization in granites. The availability of fluids that are capable of leaching uranium out of the source rocks and forces to drive significant volumes of them through the sites of mineralization is critical. The capacity of the fluids to extract and transport uranium depends on the composition of the fluids, especially with respect to oxygen fugacity and temperature, whereas the driving forces of fluid flow may be related to gravity, deformation (especially faulting), and thermally induced fluid buoyancy. Based on the similarities of the granite-related uranium mineralization systems in Beaverlodge and South China, it is proposed that basinal fluids from the red bed basins

are the main source of the mineralizing fluids, whereas extensional faulting and unevenly distributed elevated geothermal gradients related to mafic magmatism provide the essential driving forces for fluid flow. It is the coupling of these shallow (red bed basins) and deep-seated (mantle-derived magmatism) geologic processes in an extensional tectonic setting that provides the favorable conditions for uranium mineralization, as illustrated in Fig. 10 and discussed below.

Unlike meteoric fluid infiltrating the granites directly from the surface, which may be relatively limited depending on season and weather, the red bed basins may have acted as huge reservoirs which could store and supply large amounts of oxidizing fluids all the time. Furthermore, the relatively high permeabilities within the red bed basins and the oxidizing conditions as reflected by the development of Fe oxides (which are responsible for the red color of the sediments), provide favorable conditions for uranium extraction within the basins, as invoked for the Athabasca Basin and associated unconformity-related uranium deposits (Fayek and Kyser, 1997; Chi et al., 2019) and the Cretaceous – Tertiary basins in South China (Zhang et al., 2019). In the case of the Martin Lake Basin in the Beaverlodge district, basinal brines resulting from subaerial evaporation may have been developed; such fluids may evolve into the H₂O-NaCl-CaCl₂ composition due to reaction with Ca-rich minerals within the basin and/or after infiltrating the basement. The elevated densities of the basinal brines also facilitate their infiltration into the basement (Koziy et al., 2009). In the case of South China, there appears to be no widespread development of basinal brines in the red bed basins, and the basinal fluids remain at low salinities after entering the basement.

However, the availability of basinal fluids in the red bed basins alone is apparently not sufficient for creating significant uranium mineralization, as reflected by the paucity of uranium deposits around most red bed basins. The extensional tectonic setting provides an overall favorable condition for the infiltration of basinal fluids into the basement, as proposed by Chi and Zhou (2012) for the uranium mineralization in South China, but there must be some mechanisms that focus the fluid flow in particular faults or fracture zones, such as pre-existing deformation zones that may be preferably reactivated in an extensional environment. The development of fluid boiling or immiscibility in the uranium deposits both in Beaverlodge and South China suggests that fluid pressure drop associated with faulting may have played an important role in enhancing basinal fluid infiltration as depicted in the seismic pump model (Sibson, 1987) (Fig. 10). It should be noted, however, that faulting and related pressure drop may also attract fluids from other sources, including those rich in CO₂, which may further enhance the capacity of the fluid to transport uranium (Hu et al., 2008).

On the other hand, faulting is a relatively short-lived event, and it may not be sufficient to drive the amounts of fluids required to form the uranium deposits. After fluid pressure returns to the pre-faulting level, fluid flow may continue in the form of fluid convection, and some faults or fracture zones may be the paths for upward or egress flow, whereas others may act as the paths for fluid recharge or ingress flow (Fig. 10). Fluid-rock reactions in different parts of the convection loops may either extract uranium from the rocks into the fluid or precipitate uranium out of the fluid (mineralization), depending on the local physicochemical conditions. Mixing of fluids from various sources may also take place in different parts of the convection cells, and some fluid interactions (e.g. redox reactions) may further contribute to the precipitation of uranium minerals. It is important to note that although most of the ore-controlling structures are steep or subvertical, the convection model requires that these structures be connected by relatively gently dipping structures (Fig. 10). Such structures may have been formed in a compressive regime prior to the development of the extensional setting, further supporting the notion that the switch from a compressive to an extensional deformational regime is favorable for mineralization.

The fluid convection may have been enhanced by regionally

elevated geothermal gradients due to deep-seated geodynamic processes, such as asthenospheric upwelling and lithospheric thinning, as manifested by the mafic magmatism. Furthermore, the inferred increase in geothermal gradient is likely to have been unevenly distributed, and thus locally abnormal geothermal gradients may be developed (e.g., above the magma chamber feeding the mafic dikes), which would enhance egress flow in fracture zones in the vicinity of the heat source, and ingress flow in areas away from the heat source (Fig. 10). It is interesting to note that fluid-rock reactions may further contribute to the driving force of fluid flow (Bons et al., 2014). For example, fluid-rock reactions that consume water and other volatiles, such as illitization and carbonatization, would tend to draw fluids toward the sites of alteration (and mineralization), further enhancing fluid convection. The actual contribution of these fluid-rock reactions, however, depends on local geology including rock types and fluid compositions.

5. Conclusions

Based on a review of the geological setting, geological characteristics of mineralization, mineralization age, fluid composition and P-T condition, and mineralization models for the granite-related uranium mineralization in the Beaverlodge district (Canada) and South China, it is shown that the uranium mineralization in both areas have a number of similarities, which implies that they may have been controlled by similar geological factors. Among the many similarities, the most important include: 1) the uranium deposits are close to, or hosted by, granites, but the mineralization ages are much younger than the granites; 2) the mineralization is spatially associated with red bed basins and temporally overlap the development of these basins and related coeval mafic magmatism; 3) the mineralization fluids are not magmatic-hydrothermal fluids derived directly from the granites, but are basinal fluids possibly derived from the red bed basins plus fluids of various other sources; 4) the mineralization is controlled by steep faults or fracture zones that have experienced a change from a compressive to an extensional stress regime; and 5) the mineralization took place in a regional extensional tectonic setting possibly related to lithospheric thinning and asthenosphere upwelling. Both the development of the red bed basins, which provided oxidizing basinal fluids favorable for uranium extraction and transport, and the mantle-derived magmatism produced by the extensional stress regime, which provided the thermal energy for fluid circulation, are important for uranium mineralization. It is the coupling of these shallow and deep-seated geologic processes that provided the favorable conditions for uranium mineralization.

Declaration of Competing Interest

The authors declare that they have no known competing financial interests or personal relationships that could have appeared to influence the work reported in this paper.

Acknowledgements

This project is supported by an NSERC-Discovery grant (to Chi) and grants from the Saskatchewan Ministry of the Economy – Saskatchewan Geological Survey (to Chi and Ashton) for two M.Sc. theses in the Beaverlodge district. Support for the study of uranium mineralization in South China comes from a startup grant from East China University of Technology (# 2400100006) and an NSFC grant (#41930428). Constructive reviews by two anonymous reviewers greatly improved the paper.

Appendix A. Supplementary data

Supplementary data to this article can be found online at <https://doi.org/10.1016/j.oregeorev.2020.103319>.

References

- Ashton, K.E., Boivin, D., Heggie, G., 2001. Geology of the southern Black Bay Belt, west of Uranium City, Rae Province. Summary of Investigation 2001. Saskatchewan Geological Survey, Saskatchewan Energy and Mines, Miscellaneous Report 2001-4 (pp. 50-63).
- Ashton, K.E., Chi, G., Rayner, N., McFarlane, C., 2013. Geological history of granitic rocks hosting uranium mineralization in the Ace-Fay-Verna-Dubyna mines area, Beaverlodge uranium district. Summary of Investigations 2013. Saskatchewan Geological Survey, Saskatchewan Energy and Mines, Miscellaneous Report 2013-4, p. 23.
- Ashton, K.E., Card, K., Rayner, N., 2018. A New U-Pb Age for the Hudson Granites and Lamprophyre Dykes in the Southern Rae Province of Saskatchewan. Summary of Investigation 2018. Saskatchewan Geological Survey, Saskatchewan Energy and Mines, Miscellaneous Report 2018-4.2, Paper A-6, p.15.
- Ashton, K.E., Hartlaub, R.P., Heaman, L.M., Morelli, R., Bethune, K.M., Hunter, R.C., 2009. Post-Taltson sedimentary and intrusive history of the Rae Province along the northern margin of the Athabasca Basin: Western Canadian Shield. *Precamb. Res.* 175, 16–34.
- Ashton, K.E., Hartlaub, R.P., Bethune, K.M., Heaman, L.M., Rayner, N., Niebergall, G.R., 2013b. New depositional age constraints for the Murmac Bay group of the southern Rae craton, Canada. *Precamb. Res.* 232, 70–88.
- Ashton, K.E., 2010. The Gunnar mine: an episyenite-hosted, granite-related uranium deposit in the Beaverlodge uranium district. Summary of Investigation 2010. Saskatchewan Geological Survey, Saskatchewan Energy and Mines, Miscellaneous Report 2010-4, p. 21.
- Beck, L.S., 1986. General geology and uranium deposits of the Beaverlodge district. In: Evans, E.L. (Ed.), *Uranium Deposits of Canada*. C.I.M.M. Spec., pp. 85–94.
- Beck, L.S., 1969. Uranium deposits of the Athabasca Region, Saskatchewan. Saskatchewan Department of Mineral Resources, Report 1969-126, p. 139.
- Berman, R.G., Sanborn-Barrie, M., Stern, R.A., Carson, C.J., 2005. Tectonometamorphism at ca. 2.35 and 1.85 Ga in the Rae Domain, western Churchill Province, Nunavut, Canada: insights from structural, metamorphic and in situ geochronological analysis of the southwestern Committee Bay Belt. *Can. Mineral.* 43, 409–442.
- Berman, R.G., Davis, W.J., Pehrsson, S., 2007. Collisional Snowbird tectonic zone resurrected: growth of Laurentia during the 1.9 Ga accretionary phase of the Hudsonian orogeny. *Geology* 35, 911–914.
- Berman, R.G., Pehrsson, S., Davis, W.J., Ryan, J.J., Qui, H., Ashton, K.E., 2013. The Arrowsmith orogeny: geochronological and thermobarometric constraints on its extent and tectonic setting in the Rae craton, with implications for pre-Nuna supercontinent reconstruction. *Precamb. Res.* 232, 44–69.
- Bethune, K.M., Berman, R.G., Ashton, K.E., Rayner, N., 2013. Structural, petrological and U-Pb SHRIMP geochronological study of the western Beaverlodge domain: implications for crustal architecture, multi-stage orogenesis and the extent of the Taltson orogen in the SW Rae craton, Canadian Shield. *Precamb. Res.* 232, 89–118.
- Bonnetti, C., Liu, X., Mercadier, J., Cuney, M., Delouie, E., Villeneuve, J., Liu, W., 2018. The genesis of granite-related hydrothermal uranium deposits in the Xiaozhuang and Zhuguang ore fields, North Guangdong Province, SE China: insights from mineralogical, trace elements and U-Pb isotopes signatures of the U mineralisation. *Ore Geol. Rev.* 92, 588–612.
- Bons, P.D., Fusswinkel, T., Gomez-Rivas, E., Markl, G., Wagner, T., Walter, B., 2014. Fluid mixing from below in unconformity-related hydrothermal ore deposits. *Geology* 42, 1035–1038.
- Bridge, N.J., Banerjee, N.R., Pehrsson, S., Fayek, M., Finnigan, C.S., Ward, J., Berry, A., 2013. Lac Cinquante Uranium Deposit, western Churchill Province, Nunavut, Canada. *Explor. Mining Geol.* 21, 27–50.
- Card, C.D., Pana, D., Portella, P., Thomas, D.J., Annesley, I.R., 2007. Basement rocks of the Athabasca Basin, Saskatchewan, and Alberta. *Geol. Surv. Canada Bull.* 588, 69–87.
- Carter, A., Clift, P.D., 2008. Was the Indosinian orogeny a Triassic mountain building or a thermotectonic reactivation event? *C.R. Geoscience* 340, 83–93.
- Charvet, J., Shu, L., Shi, Y., Guo, L., Faure, M., 1996. The building of south China: collision of Yangzi and Cathaysia blocks, problems and tentative answers. *J. Asian Earth Sci.* 13, 223–235.
- Charvet, J., Shu, L., Faure, M., Choulet, F., Bo, W., Lu, H., 2010. Structural development of the Lower Paleozoic belt of South China: genesis of an intracontinental orogen. *J. Asian Earth Sci.* 39, 309–330.
- Chen, G.D., 1956. Examples of “activated region” in Chinese Platform with special reference to the “Cathaysia” problem. *Acta Geol. Sin.* 36, 239–272 (in Chinese with English abstract).
- Chi, G., Zhou, Y., 2012. Hydrodynamic constraints on relationships between different types of U deposits in southern China. *Mineralogical Magazine, Goldschmidt 2012 Conference Abstracts*, p. 1573.
- Chi, G., Chu, H., Petts, D., Potter, E., Jackson, S., Williams-Jones, A.E., 2019. Uranium-rich diagenetic fluids provide the key to unconformity-related uranium mineralization in the Athabasca Basin. *Sci. Rep.* 9 (5530), 1–10. <https://doi.org/10.1038/s41598-019-42032-0>.
- Dahlkamp, F.J., 2009. *Uranium Deposits of the World – Asia*. Springer, pp. 493.
- Deng, P., Shu, L.S., Tan, Z.Z., 2003. The geological setting for the formation of rich uranium ores in the Zhuguang-Guidong large-scale uranium metallogenetic area. *Geol. Rev.* 49, 486–494 (in Chinese with English abs.).
- Deng, T., Xu, D., Chi, G., Wang, Z., Chen, G., Li, Z., Zhang, J., Ye, T., Yu, D., 2019. Revisiting the ca. 845–820 Ma S-type granitic magmatism in the Jiangnan Orogen: New insights on the Neoproterozoic tectono-magmatic evolution of South China. *Int. Geol. Rev.* 61, 383–403.
- Dieng, S., Kyser, K., Godin, L., 2013. Tectonic history of the North American shield recorded in uranium deposits in the Beaverlodge area, northern Saskatchewan, Canada. *Precamb. Res.* 224, 316–340.
- Dieng, S., Kyser, K., Godin, L., 2015. Genesis of multifarious uranium mineralization in the Beaverlodge area, northern Saskatchewan, Canada. *Econ. Geol.* 110, 209–240.
- Du, L., Wang, Y., 1984. The unity of mineralization mechanism of granite-type, volcanic-type, carbonaceous-siliceous-pelite-type, and sandstone-type uranium deposits. *Radioactive Geol.* 3, 1–10 (in Chinese, with English abstract).
- Evoy, E.F., 1986. The Gunnar uranium deposit. In: Evans, E.L. (Eds.), *Uranium Deposits of Canada*, *Can. Inst. Min. Metall.* 33, 250–260.
- Faure, M., Lepvrier, C., Nguyen, V.V., Vu, T.V., Lin, W., Chen, Z., 2014. The South China block – Indochina collision: Where, when, and how? *J. Asian Earth Sci.* 79, 260–274.
- Fayek, M., Kyser, T.K., 1997. Characterization of multiple fluid flow events and rare earth element mobility associated with formation of unconformity-type uranium deposits in the Athabasca Basin, Saskatchewan. *Can. Mineral.* 35, 627–658.
- Guo, F.X., 1998. On the Indosinian Movement of Southeast China. *J. Guilin Inst. Technol.* 18, 313–322 (in Chinese, with English abstract).
- Hartlaub, R.P., Heaman, L.M., Ashton, K.E., Chacko, T., 2004. The Archean Murmac Bay Group: evidence for a giant Archean rift in the Rae Province, Canada. *Precamb. Res.* 131, 345–372.
- Hartlaub, R.P., Chacko, T., Heaman, L.M., Creaser, R., Ashton, K.E., Simonetti, A., 2005. Ancient (Meso to Paleoproterozoic) crust in the Rae Province, Canada: evidence from Sm-Nd and U-Pb constraints. *Precamb. Res.* 141, 137–153.
- Hartlaub, R.P., Heaman, L.M., Chacko, T., Ashton, K.E., 2007. Circa 2.3-Ga magmatism of the Arrowsmith orogeny, Uranium City Region, Western Churchill Craton, Canada. *J. Geol.* 115, 181–195.
- Hoffman, P.E., 1988. United plates of America, the birth of a craton: early Proterozoic assembly and growth of Laurentia. *Ann. Rev. Earth Planet Sci.* 16, 543–603.
- Hu, R.Z., Bi, X.W., Zhou, M.F., Peng, J., Su, W., Liu, S., Qi, H., 2008. Uranium metallogenesis in South China and its relationship to crustal extension during the Cretaceous to Tertiary. *Econ. Geol.* 103, 583–598.
- Huang, S.X., Du, L.T., Xie, Y.X., Zhang, D.S., Chen, G., Wan, G.L., Ji, S.F., 1994. Uranium deposits in China. In: Song, S.H. (Ed.), *Mineral Deposits in China*, pp. 329–385 (in Chinese, with English abstract).
- IAEA, 2009. World distribution of uranium deposits (UDEPO) with uranium deposit classification. IAEA-TECDOC-1629, p. 117.
- IAEA, 2018. Geological classification of uranium deposits and description of selected examples. IAEA-TECDOC-1842, p. 415.
- Jefferson, C.W., Thomas, D.J., Gandhi, S.S., Ramaekers, P., Delaney, G., Brisbin, D., Cutts, C., Portella, P., Olson, R.A., 2007. Unconformity associated uranium deposits of the Athabasca Basin, Saskatchewan and Alberta. *Geol. Surv. Canada Bull.* 588, 273–305.
- Kennicott, J., Chi, G., Ashton, K., 2015. Field and petrographic study of albitization associated with uranium mineralization in the Beaverlodge uranium district of northern Saskatchewan. Summary of Investigations 2015, Saskatchewan Geological Survey, Saskatchewan Ministry of Economy, Miscellaneous Report 2015-4.2, Paper A4, p. 24.
- Koepfel, V., 1968. Age and the history of uranium mineralization of the Beaverlodge area, Saskatchewan. *Geol. Surv. Can.* 67–31, 111.
- Koziy, L., Bull, S., Large, R., Selley, D., 2009. Salt as a fluid driver, and basement as a metal source, for stratiform sediment-hosted copper deposits. *Geology* 37, 1107–1110.
- LeGault, T., 2014. *Petrographic and Geochemical Study of Hydrothermal Albitite Alteration in the Beaverlodge Uranium District, Northwestern Saskatchewan, Canada*. Unpublished B.Sc. thesis. University of Regina.
- Li, J.C., Chen, Y.L., Zhang, C.J., 2011. *Uranium Geology and Exploration*. Geological Publishing House, Beijing, pp. 190 (in Chinese).
- Li, X.H., Li, Z.X., Li, W.X., Wang, Y., 2006. Initiation of the Indosinian orogeny in South China: evidence for a Permian magmatic arc on Hainan Island. *J. Geol.* 114, 341–353.
- Li, Z., Li, X., 2007. Formation of the 1300-km-wide intracontinental orogen and post-orogenic magmatic province in the Mesozoic South China: a flat-slab subduction model. *Geology* 35, 179–182.
- Li, J., Zhang, Y., Dong, S., Johnston, S.T., 2014. Cretaceous tectonic evolution of South China: a preliminary synthesis. *Earth Sci. Rev.* 134, 98–136.
- Liang, R., Chi, G., Ashton, K., Blamey, N., Fayek, M., 2017. Fluid compositions and P-T conditions of vein-type uranium mineralization in the Beaverlodge uranium district, northern Saskatchewan, Canada. *Ore Geol. Rev.* 80, 460–483.
- Ludwig, K.R., Simmons, K.R., 1992. U-Pb dating of uranium deposits in collapse breccia pipes of the Grand Canyon Region. *Econ. Geol.* 87, 1747–1765.
- Luo, J.C., Hu, R.Z., Fayek, M., Li, C.S., Bi, X.W., Abdu, Y., Chen, Y.W., 2015. In-situ SIMS uraninite U-Pb dating and genesis of the Xianshi granite-hosted uranium deposit, south China. *Ore Geol. Rev.* 65, 968–978.
- Mao, J.W., Cheng, Y., Chen, M., Pirajno, F., 2013. Major types and time-space distribution of Mesozoic ore deposits in south China and their geodynamic settings. *Miner. Deposita* 48, 267–294.
- Mazimhaka, P.K., Hendry, H.E., 1984. The Martin Group, Beaverlodge Area. Summary of Investigations 1984. Saskatchewan Geological Survey, Saskatchewan Energy and Mines, Miscellaneous Report 1984-4 (pp. 53–62).
- Meng, Q.R., Zhang, G.W., 2000. Geologic framework and tectonic evolution of Qinling orogen, central China. *Tectonophysics* 323, 183–196.
- Min, M., Fang, C., Fayek, M., 2005. Petrography and genetic history of coffinite and uraninite from the Liueyiqi granite-hosted uranium deposit, SE China. *Ore Geol. Rev.* 26, 187–197.
- Morelli, R.M., Hartlaub, R.P., Ashton, K.E., Ansdell, K.M., 2009. Evidence for enrichment of subcontinental lithospheric mantle from Paleoproterozoic intracratonic magmas: geochemistry and U-Pb geochronology of Martin Group igneous rocks, Western Rae Craton, Canada. *Precamb. Res.* 175, 1–15.
- NEA-OECD, 2018. *Uranium 2018: Resources, Production and Demand*. A Joint Report by

- IAEA and NEA, NEA No. 7413, p. 457.
- Peterson, T.D., van Breemen, O., Sandeman, H., Cousens, B., 2002. Proterozoic (1.85-1.75 Ga) igneous suites of the Western Churchill Province: granitoid and ultrapotassic magmatism in a reworked Archean hinterland. *Precam. Res.* 119, 73–100.
- Rainbird, R.H., Davis, W.J., Pehrsson, S.J., Wodicka, N., Rayner, N., Skulski, T., 2010. Early Paleoproterozoic supracrustal assemblages of the Rae domain, Nunavut, Canada: intracratonic basin development during supercontinent break-up and assembly. *Precam. Res.* 181, 167–186.
- Ramaekers, P., McElroy, R., Catuneanu, O., 2017. Mid-Proterozoic continental extension as a control on Athabasca region uranium emplacement, Saskatchewan and Alberta, Canada. SGA Biennial Conference (Quebec, August 20–23, 2017) Proceedings, 759–762.
- Ramaekers, P., Jefferson, C.W., Yeo, G.M., Collier, B., Long, D.G., Catuneanu, O., Bernier, S., Kupsch, B., Post, R., Drever, G., McHardy, S., Jircka, D., Cutts, C., Wheatley, K., 2007. Revised geological map and stratigraphy of the Athabasca Group, Saskatchewan and Alberta. In: Jefferson, C.W., Delaney, G. (Eds.), EXTECH IV: Geology and Exploration Technology of the Proterozoic Athabasca Basin, Saskatchewan and Alberta. Geological Survey of Canada Bulletin, pp. 155–191.
- Rees, M.I., 1992. History of the Fluids Associated with Lode-gold Deposits, and Complex U-PGE-Au Vein Type Deposits, Goldfields Peninsula, Northern Saskatchewan, Canada. M.Sc. thesis. University of Saskatchewan, Saskatoon, pp. 209.
- Robinson, S.C., 1955. Mineralogy of uranium deposits, Goldfields, Saskatchewan. *Canada Geol. Survey Bull.* 31, 32–35.
- Ruzicka, V., 1993. Vein uranium deposits. In: Haynes, S.J. (Eds.), *Vein-type Ore Deposits*, *Ore Geol. Rev.* 8, 247–276.
- Sassano, G.P., Fritz, P., Morton, R.D., 1972. Paragenesis and isotopic composition of some gangue minerals from the uranium deposits of Eldorado, Saskatchewan. *Can. J. Earth Sci.* 9, 141–157.
- Shen, W., Zhang, Z., Zhang, B., 1988. A study on isotope geology of some granite type uranium deposits in South China. *Acta Geol. Sin.* 62, 51–62 (in Chinese, with English abstract).
- Shu, L., Zhou, G., Shi, Y., Yin, J., 1994. Study of the high pressure metamorphic blueschist and its Late Proterozoic age in the eastern Jiangnan belt. *Chin. Sci. Bull.* 39, 1200–1204.
- Sibson, R.H., 1987. Earthquake rupturing as a mineralizing agent in hydrothermal systems. *Geology* v. 15, 701–704.
- Smith, E.E.N., 1986. Geology of the Beaverlodge operation Eldorado Nuclear Limited SA. In: Evans E.L. (Eds.), *Uranium Deposits of Canada*, C.I.M.M. Spec. 33, 95–109.
- Sun, W.D., Ding, X., Hu, Y.H., Li, X.H., 2007. The golden transformation of the Cretaceous plate subduction in the west Pacific. *Earth Planet. Sci. Lett.* 262, 533–542.
- Tortosa, D.J.J., Langford, F.F., 1986. The geology of the Cenex U deposit, Beaverlodge, Saskatchewan. In: Evans E.L. (Eds.), *Uranium Deposits of Canada*, C.I.M.M. Spec. 33, 110–119.
- Tremblay, L.P., 1972. Geology of the Beaverlodge Mining area, Saskatchewan. *Geol. Surv. Can. Mem.* 367, 265p.
- Tremblay, L.P., 1978. Geologic setting of the Beaverlodge-type vein-uranium deposit and its comparison to that of the unconformity-type; *Miner. Assoc. Can. Short Course Handbook* 3, 431–456.
- Wang, J., Li, Z.X., 2003. History of Neoproterozoic rift basins in South China: implications for Rodinia break-up. *Precam. Res.* 122, 141–158.
- Wang, M., Luo, Y., Sun, Z., 1999. Discussion on genesis of uranium deposits in Zhuguang uranium metallogenic region. *Uranium Geol.* 15, 279–285 (in Chinese, with English abstract).
- Wang, Z., Zhou, X., Zeng, D., Wang, G., Teng, R., 2002. Metallogenic model for Mesozoic unconformity-related uranium deposits in South China. *Geol. Rev.* 48, 365–371 (in Chinese, with English abstract).
- Wong, W.H., 1927. Crustal movements and igneous activities in eastern China since Mesozoic time. *Acta Geol. Sin.* 6, 9–37.
- Xia, Z., Li, W., Fan, H., Pang, Y., Zhang, M., 2016. Geological features and metallogenic model of granite-peripheral uranium deposits in overlying basins in South China. *Uranium Geol.* 32, 99–103 (in Chinese, with English abstract).
- Xu, D., Chi, G., Zhang, Y., Zhang, Z., Sun, W., 2017. Yanshanian (Late Mesozoic) ore deposits in China – an introduction to the special issue. *Ore Geol. Rev.* 88, 481–490.
- Zhang, Z., 1989. On the mutual relationship between the principal types of uranium deposits in SE China. *Chin. J. Nucl. Sci. Eng.* 9, 162–169.
- Zhang, C., Cai, Y., Xu, H., Liu, J., 2016. Mineralization mechanism of No. 302 uranium deposit, northern Guangdong Province: evidence from fluid inclusions. *J. East China Univ. Technol.* 39, 156–164 (in Chinese, with English abstract).
- Zhang, C., Cai, Y., Xu, H., Liu, J., Hao, R., 2017. Mechanism of mineralization in the Changjiang uranium ore field, south China: evidence from fluid inclusions, hydrothermal alteration, and H-O isotopes. *Ore Geol. Rev.* 86, 225–253.
- Zhang, C., Cai, Y., Dong, Q., Xu, H., 2019. Cretaceous – Neogene basin control on the formation of uranium deposits in South China: evidence from geology, mineralization ages, and H-O isotopes. *Int. Geol. Rev.* <https://doi.org/10.1080/00206814.2019.1598898>.
- Zhao, G., Cawood, P.A., 2012. Precambrian geology of China. *Precam. Res.* 222, 13–54.
- Zheng, Y., Wu, R., Wu, Y., Zhang, S., Yuan, H., Wu, F., 2008. Rift melting of juvenile arc-derived crust: geochemical evidence from Neoproterozoic volcanic and granitic rocks in the Jiangnan Orogen, South China. *Precam. Res.* 163, 351–383.
- Zhou, X.M., Sun, T., Shen, W.Z., Shu, L.S., Niu, Y.L., 2006. Petrogenesis of Mesozoic granitoids and volcanic rocks in South China: a response to tectonic evolution. *Episodes* 29, 26–33.
- Zhou, J., Wang, X., Qiu, J., 2009. Geochronology of Neoproterozoic mafic rocks and sandstones from northeastern Guizhou, South China: coeval arc magmatism and sedimentation. *Precam. Res.* 170, 27–42.
- Zhu, R.X., Yang, J.H., Wu, F.Y., 2012. Timing of destruction of the North China Craton. *Lithos* 149, 51–60.